Measure-preserving and Time-reversible Integration Algorithms for Constant Temperature Molecular Dynamics.

by

Emmanuel Omboga Obaga

Submitted in fulfillment of the requirements

for the degree of Master of Science in the

School of Physics,

UNIVERSITY OF KWAZULU-NATAL

Pietermaritzburg

December, 2011

Abstract

This thesis concerns the formulation of integration algorithms for non-Hamiltonian molecular dynamics simulation at constant temperature. In particular, the constant temperature dynamics of the Nosé-Hoover, Nosé-Hoover chain, and Bulgac-Kusnezov thermostats are studied. In all cases, the equilibrium statistical mechanics and the integration algorithms have been formulated using non-Hamiltonian brackets in phase space. A systematic approach has been followed in deriving numerically stable and efficient algorithms. Starting from a set of equations of motion, time-reversible algorithms have been formulated through the time-symmetric Trotter factorization of the Liouville propagator. Such a time-symmetric factorization can be combined with the underlying non-Hamiltonian bracket-structure of the Liouville operator, preserving the measure of phase space. In this latter case, algorithms that are both time-reversible and measure-preserving can be obtained. Constant temperature simulations of low-dimensional harmonic systems have been performed in order to illustrate the accuracy and the efficiency of the algorithms presented in this thesis.

Preface

All the work / numerical experiments / analysis presented in this thesis are the results of the collaborative effort within the School of Physics, University of KwaZulu-Natal, Pietermaritzburg, from January 2010 to December 2011, under the supervision of Dr. Alessandro Sergi.

Declaration

I declare that this work is a result of my own research, except where specifically indicated to the contrary and references duly acknowledged, has not been submitted for any other degree or examination to any other tertiary institution.

Student :_____ Date : _____

E. Obaga

Supervisor : Alemendo Sergi Date : March 29, 2012

Dr. A. Sergi

Acknowledgments

With the completion of two years of hard work, I now come to the end, and perhaps the most difficult, but pleasant, part of acknowledging all of the family, supervisor, academic staff, friends and colleagues that have been crucial in keeping me focused throughout my time as a postgraduate student. Their love, patience, and encouragement have immensely helped me in completion of this thesis.

First and foremost, I would like to express my eternal gratitude to my supervisor Dr. Alessandro Sergi. He has always been eager to listen and provide help and advice. His mastery of the subject, enthusiasm and tireless efforts are unsurpassed. Being more than an academic adviser he has been a great source of inspiration to me. His ever presence, patience, understanding, kindness and genuine friendship has made my research under his close supervision excitingly enjoyable. It is through his guidance and helpful discussions that I was able to piece this puzzle together. In this connection I am now most pleased to say that the secret of my project success started when I selected Dr. Alessandro Sergi as my supervisor.

My heartfelt gratitude and respect goes to my parents, Samuel and Jemmimah Obaga, for their unconditional support and unwavering confidence throughout the past years. There are simply no words to express fully the influence my family has had on me, both as a student and as a person. All through I have

enjoyed the full trust of my mother and father, who have always given me every opportunity to achieve as high as possible. Their selfless love, genuine friendship, substantial financial support, constant care and undying interest in everything I am doing, has made me into the man I am today. Mum and dad, I hope this makes you proud.

Staff at University of KwaZulu-Natal in the school of physics have been most helpful, and have always ensured that things run smoothly for me during the seven years I have spent here as a student and this has been greatly appreciated.

I would also like to thank my other colleagues and fellow students. While I cannot write about them individually, each of them has been important to me at various stages throughout my time at the university.

I must extend a big thank you to Dr.Robert Lindebaum and Dr. Naven Chetty for their valuable guidance, and University of KwaZulu-Natal for facilitating my six months contract as a Tutor in Augmented Physics, which greatly enhanced my rich appreciation of the beauty of physics in addition to affording me vital exposure and development of necessary skills on the handling of Physics.

Contents

List of Figures

List of Tables

Chapter 1

Introduction

In the early 1950s, different types of computer simulation techniques developed were purposely used in military experiments such as nuclear weapon development[1]. The research carried out primarily used and implemented the Monte Carlo simulation[2] technique. This type of simulation is a stochastic process which in general is very powerful but does not permit easy calculation of time-dependent properties. To overcome this limitation, a new method was developed in the 1960s which had the capabilities of allowing the calculation of time-dependent quantities. This method known as molecular dynamics (MD in short) [1, 2, 3], is deterministic in nature. This thesis shall concern itself with algorithms for performing MD simulations at constant temperature.

MD in essence is a type of simulation technique for computing the equilibrium and transport properties of a system of particles[1, 2, 3]. The basic form of the original formulation of MD follows Hamiltonian dynamics. Given appropriate boundary conditions specific to the symmetry or geometry of the system, the time-dependent behavior of the constituent particles can be followed through numerical integration of their equations of motion[1, 2, 3]. The calculation of position and momenta[2] of the particle for each instant of time defines the

trajectory in phase space. Furthermore, the description of the inter-particle interacting potential[2] affects the accuracy and quality of the results.

Time averages obtained by MD correspond to the microcanonical ensemble of Statistical mechanics. This connection is made possible using the ergodic hypothesis. Real experiments are very often carried out at isothermal conditions[4]. Thus, results obtained through numerical simulations can be compared with real ones if one performs the calculations in the canonical ensemble. In the thermodynamic limit, different ensembles are equivalent[4]. However, it is difficult to achieve this limit when performing calculations under real-life conditions and thus differences emerge between constant enthalpy Hamiltonian MD results and those produced by constant temperature dynamics.

It is well known that in principle a canonical representation of the system of interest coupled to a heat bath can be achieved within a constant energy scheme. The heat bath in this case is represented using an infinite number of degrees of freedom. Due to the limited computational resources available, the infinite conditions can not be simulated in a computer and as such several proposals[5] have been put forward to overcome this limitation. One such proposal within constant temperature MD was introduced by Nosé[6, 7, 8, 9] in the 1980s. Nosé further built on the extended systems approach that was first proposed by Andersen to perform constant pressure MD[5, 10]. The extended systems approach is characterized by non-Hamiltonian dynamics [11] that conserves energy in the extended phase space [5].

In recent years, the extended systems dynamics[5] paved the way for deriving a number of different equations of motion that conserve a generalized energy function[12]. Moreover, the same phase space[13, 14] distribution function is achieved using different equations of motion. Following the work of Sergi and Ferrario [5], it is shown that an underlying unique general mathematical structure exists for the non-Hamiltonian equations of motion using the symplectic

form of Hamilton's equations. From this generalized structure one can select the compressibility of phase space and obtain an ensemble distribution for the physical system of interest for a given conserved Hamiltonian. It has been shown[5] recently how the invariant measure of phase space is formulated using the compressibility within non-Hamiltonian dynamics.

In the work of Sergi and Ferrario [5], non-Hamiltonian flows that sample the phase space in line with a chosen distribution function have been derived. Moreover, a new algebraic bracket was formalized by Sergi [15] for non-Hamiltonian systems in equilibrium statistical mechanics. Given a proper bracket one can find the Liouville operator. Within the Trotter formalism[16, 17, 18], Tuckerman *et al*[16] derived time-reversible algorithms using a symmetric Trotter factorization of the Liouville propagator. Ezra[19, 20] using explicitly the bracket structure of the Liouville operator was able to improve on the approach of Tuckerman *et al* [16] and produced algorithms which are both time-reversible and measure-preserving.

In this thesis we set out to accomplish the following goals; First, we reformulate the dynamics for the Nosé-Hoover, Nosé-Hoover chain and Bulgac-Kusnezov thermostats using non-Hamiltonian brackets in phase space[5, 15]. Second, we show how to systematically derive stable and efficient time-reversible and reversible measure-preserving algorithms for all the above phase space flows. The approach towards this method was recently introduced based on the underlying mathematical structure of non-Hamiltonian phase space[20]. Finally, using a paradigmatic example of a one-dimension oscillator, we present and discuss numerical results for the Nosé-Hoover chain and Bulgac-Kusnezov thermostats.

The organization of this thesis is as follows. In chapter 2, an introduction to MD is presented and explained, and a connection to statistical mechanics given. Moreover, a commonly used method for integrating MD equations of motion is also presented within the chapter. In chapter 3, we introduce the

generalized algebraic bracket used in non-Hamiltonian dynamics. In chapter 4, we derive the time-reversible and measure-preserving algorithms for the following deterministic thermostats; Nosé-Hoover, Nosé-Hoover chain and the Bulgac-Kusnezov. In chapter 5, we investigate different models using the simple harmonic oscillator. Finally, in chapter 6, we give a conclusion to the findings.

In addition several appendices have been included. A complete derivation for a useful operator formula is shown in appendix A. Appendix B shows the derivation of the invariant measure of the Nosé-Hoover, Nosé-Hoover chain and Bulgac-Kusnezov phase space flows. Finally, the Liouville operator for the Nosé-Hoover, Nosé-Hoover chain and Bulgac-Kusnezov dynamics is derived in Appendix C.

Chapter 2

Molecular dynamics

In this chapter I give a brief overview of the fundamental approach used in defining a system mathematically within MD simulation. Also, I shall discuss the connection between MD and statistical mechanics and show a widely used algorithm implemented when integrating the equations of motion under MD.

2.1 Introduction

The method of simulating the dynamics of a system of particles or fields[19] using a computer is what is referred to as molecular dynamics (MD)[1, 2, 3]. From a conceptual perspective, MD simulations can be considered as numerical experiments, in many respects similar to real ones. This idea can be further clarified using the following analogy [1]. When performing real experiments, the following steps are followed; The sample of the material of interest is prepared. Using a measuring instrument (such as a thermometer or barometer) during certain time interval, the property of interest of the sample is measured. For greater accuracy, averages over a long period of time have to be taken in order to diminish the statistical noises[1]. In the case of MD simulations, the

approach is similar. The sample to be prepared is generally a system consisting of a set of N interacting particles whose dynamical evolution is followed through numerical integration of Newton's equations of motion. Using appropriate boundary conditions specific to the geometry or symmetry of the system, the calculation of the system's properties takes the place in the simulation of the measurements in the experiments. Moreover, averages are taken after the system has been properly equilibrated.

The microscopic behavior of a system can be studied using the laws of classical mechanics given that an inter-particle interaction potential (or force field) is given. Through MD simulations the information that we obtain on the system is given by the particles position and momenta [1, 2] which define the trajectory in phase space. Once the phase space trajectory is known averages in phase space provides the connection to macroscopic quantities. The macroscopic observables in this case are quantities such as temperature and pressure. Statistical mechanics[2] provides the necessary connection between the macroscopic observables and the microscopic properties.

The application of MD technique is vast as it is applicable to a wide variety of problems in many branches of science such as chemistry, astrophysics and condensed matter physics[1, 21, 22, 23, 24].

2.2 Basic approach

The application of MD to a variety of problems is technically based on the following important elements. Initial conditions are chosen obeying a specified thermodynamic constraints in a stochastic way from the correct probability distribution function[19] in phase space. Also, forces can be calculated by a careful choice of the interaction potential[2, 19]. The numerical integration of the equations of motion allows one to follow the dynamical evolution [2, 19]

of the system. The trajectory is generated through solving Newton's classical equations of motion

$$F_i = m_i a_i, \tag{2.2.1}$$

where i is an index corresponding to each particle coordinate within a system constituted by a certain number of atoms. Here, F_i is the force acting upon an atom due to its interaction with the other atoms, m_i is its mass and a_i is the acceleration. Equivalently, one can integrate the classical Hamilton's equation of motion[2, 4] :

$$\begin{bmatrix} \dot{q}_i \\ \dot{p}_i \end{bmatrix} = \begin{bmatrix} 0 & 1 \\ -1 & 0 \end{bmatrix} \cdot \begin{bmatrix} \frac{\partial H}{\partial q_i} \\ \frac{\partial H}{\partial p_i} \end{bmatrix}, \tag{2.2.2}$$

where p_i and q_i are the momentum and position coordinates for the i^{th} atomic coordinate.

The Hamiltonian (energy function), H, is given as a sum of the kinetic and potential energy functions of the set of N coordinates q_i and N momenta p_i of each molecule. Usually the kinetic energy takes the form of $\frac{p_i^2}{2m_i}$ where m_i is the mass of the molecule and p_i is its conjugated momenta, and the potential energy written in general as $V(q_1, q_2, \ldots, q_N) = V(q)$ contains information about the intermolecular interactions and is given as a function of all particles position q_i. The coordinate q_i and momenta p_i collectively define the phase space of the system (q, p). For a particular system, the Hamiltonian may be represented as

$$H = \sum_{i=1}^{N} \frac{p_i^2}{2m_i} + V(q). \tag{2.2.3}$$

The force on an atom can be calculated as the derivative of energy with respect to the change in the atom's position[2]

$$F_i = -\nabla_i V = -\frac{dE}{dq_i}. \tag{2.2.4}$$

Using available information about the atomic forces and masses, the positions of each atom can be solved along a series of infinitesimal time steps[2]. Once the force is known one can use various numerical algorithms to integrate the equations of motion.

To summarize the entire procedure, at each time step, the forces on the atoms are calculated and combined with the current phase space coordinates (q, p) to generate a new set of coordinates (q, p) a short time step ahead. The atoms are then moved to the new coordinates, the forces are recalculated and the new dynamic cycle goes on. For a clearer observation, such an algorithm has been represented diagrammatically in Fig. 2.1 [4].

The equations of motion have two important properties. The first one is that they are time reversible[2], that is, when the transformation $t \to -t$ is made the equations of motion retain the same form and as a consequence of this property the microscopic properties are independent of the direction of flow of time[2]. The second property is that they conserve the Hamiltonian. This can be easily seen by computing the time derivative of H and substituting (2.2.2) for the time derivatives of position and momentum[2]

$$\frac{dH}{dt} = \sum_{i=1}^{N}\left[\frac{\partial H}{\partial q}\dot{q}_i + \frac{\partial H}{\partial p_i}\dot{p}_i\right] = \sum_{i=1}^{N}\left[\frac{\partial H}{\partial q_i}\frac{\partial H}{\partial p_i} - \frac{\partial H}{\partial p_i}\frac{\partial H}{\partial q_i}\right] = 0 \tag{2.2.5}$$

The conservation of the Hamiltonian[2] provides an important connection between MD and statistical mechanics since it is equivalent to the conservation

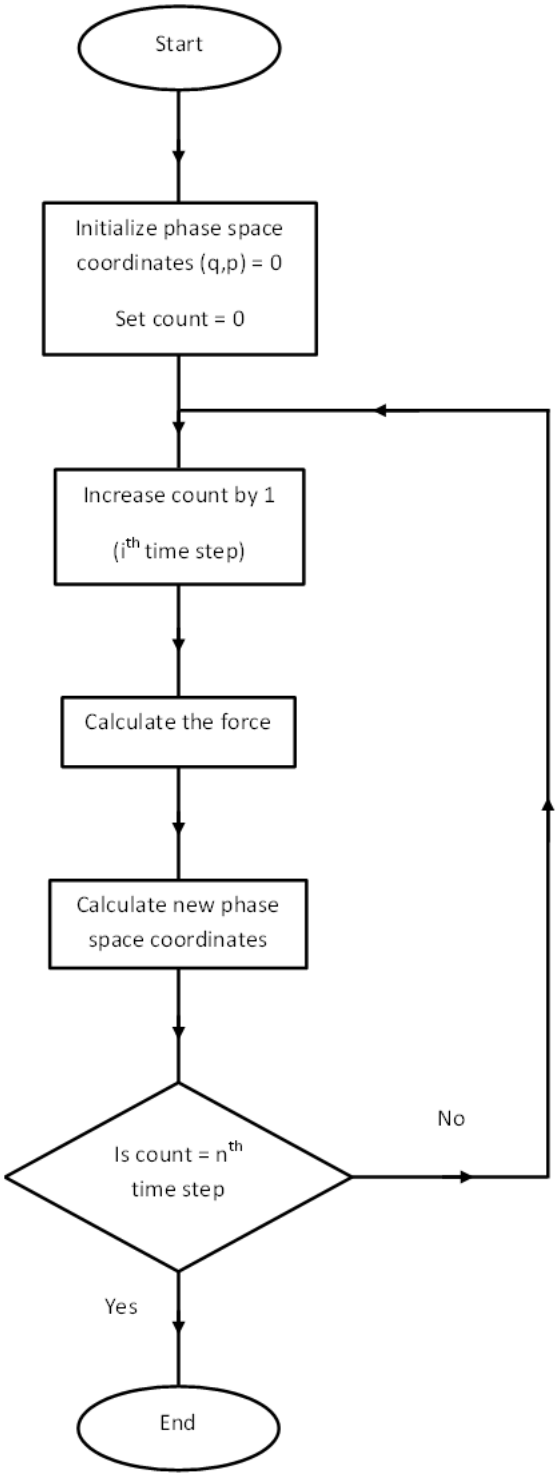

Fig. 2.1: Flowchart diagram showing the various steps in calculating a new set of phase space coordinates from a set of initial conditions.

of the total energy of the system.

2.3 Relation to statistical mechanics

When performing calculations by MD simulation techniques, one typically follows a particles phase space trajectory given by its position and momenta. Such information describes the microscopic properties specific to the system of interest and can be related to macroscopic observables (pressure, internal energy, etc.) through statistical mechanics[2]. Consider a system of N particles with a dynamical quantity, say A, with $\mathbf{x}$ being points in phase space computed along the total time interval T, the time averages are given in the form

$$\langle A \rangle_{time} = \lim_{T \to \infty} \frac{1}{T} \int_0^T dt\, A\left(\mathbf{x}\left(t\right)\right). \tag{2.3.1}$$

The equations of motion that govern the above equation are a set of ordinary differential equations that are described in classical systems by Newton's equations of motion. Such equations can be solved numerically using a computer. However, one encounters several problems when carrying out these simulations. For instance one would simulate a system consisting of a finite number of particles (e.g 10^3) as opposed to a system with a truly macroscopic number (e.g 10^{23})[25], this is due to limited available computational resources. Also, when obtaining time averages using equation (2.3.1), the integration scheme can not be performed for an infinite amount of time. Thus, the question that now arises is whether or not a particle's trajectory has explored sufficiently regions of phase space to yield satisfactory time averages within a feasible amount of computer time[25]. Also, using different initial conditions, the accuracy of different simulations with identical macroscopic parameters (density, energy etc.)

can be tested for thermodynamic consistencies. Answers to such questions lie through the careful choices of the integration method schemes which are looked at further within the thesis.

Due to the complexity of the time evolution of the dynamical quantity $A(\mathbf{x}, t)$ for a large number of particles, Gibbs [25] proposed the replacement of time-averages with ensemble averages. Gibbs statistical mechanics uses ensemble averages in obtaining the thermodynamic properties as opposed to the calculation of time averages implied in MD simulations. The ensemble in this case is regarded as a collection of points $\mathbf{x}$ in phase space distributed according to a chosen probability function $\rho(\mathbf{x})$. This phase space points define a particular system at an instant of time. Following a set of equations of motion, each system can evolve independently in time. As a result, the probability function $\rho(\mathbf{x})$ also changes in time. However, according to Liouville's theorem, the probability distribution function of a system is a constant of time[25], that is,

$$\frac{d}{dt}\rho(\mathbf{x}) = 0. \tag{2.3.2}$$

Thus, suppose a system is defined with N number of particles and a specific distribution function $\rho(\mathbf{x})$ where $\mathbf{x}$ is the generalized coordinates (q, p_i), q and p denote the positions and momenta respectively. The total time derivative of $\rho(\mathbf{x})$ is

$$\frac{d}{dt}\rho(\mathbf{x}) = \frac{\partial}{\partial t}\rho(\mathbf{x}) + \sum_{i=1}^{N} \dot{q}_i \frac{\partial}{\partial q_i}\rho(\mathbf{x}) + \sum_{i=1}^{N} \dot{p}_i \frac{\partial}{\partial p_i}\rho(\mathbf{x}). \tag{2.3.3}$$

The Liouville operator L can be defined as

$$iL = \sum_{i=1}^{N} \left(\dot{q}_i \frac{\partial}{\partial q_i} + \dot{p}_i \frac{\partial}{\partial p_i} \right). \tag{2.3.4}$$

Thus, equation (2.3.3) can be re-written as

$$\frac{d}{dt}\rho\left(\mathbf{x}\right)=\frac{\partial}{\partial t}\rho\left(\mathbf{x}\right)+iL\rho\left(\mathbf{x}\right), \tag{2.3.5}$$

and using Liouville's theorem[19], we may write

$$\frac{\partial}{\partial t}\rho\left(\mathbf{x}\left(t\right)\right)=-iL\rho\left(\mathbf{x}\left(t\right)\right). \tag{2.3.6}$$

Where the formal solution to the above equation is given by

$$\rho\left(\mathbf{x}\left(t\right)\right)=exp\left(-iLt\right)\rho\left(\mathbf{x}\left(0\right)\right). \tag{2.3.7}$$

For the dynamical function $A\left(\mathbf{x},t\right)$ the equations of motion, which are explicitly time independent, take the form

$$\dot{A}\left(\mathbf{x},t\right)=iLA\left(\mathbf{x},t\right) \tag{2.3.8}$$

or

$$A\left(\mathbf{x},t\right)=exp\left(iLt\right)A\left(\mathbf{x},0\right) \tag{2.3.9}$$

Within statistical mechanics equations (2.3.6) and (2.3.7) describe the Schrödinger picture[26] since we consider the time-dependence of ρ at a fixed point in phase space whereas equations (2.3.8) and (2.3.9) represent the Heisenberg picture since the dynamical function $A\left(\mathbf{x},t\right)$ evolves with time as the trajectory of the phase space point $\mathbf{x}$ is followed throughout the time evolution.

If for an equilibrium ensemble, $\partial\rho/\partial t=0$, and there exists a trajectory which passes throughout all the phase space points for which $\rho\neq0$ then each system

will eventually access all the regions of phase space. The ensemble average for all the states of the system is given by

$$\langle A \rangle = \int dx^{2N} \rho\left(\mathbf{x}\right) A\left(\mathbf{x},t\right). \tag{2.3.10}$$

Assuming that the limit $T \to \infty$ for equation (2.3.1) is numerically achieved and that the sampling for equation (2.3.10) is sufficiently thorough, then one can invoke the ergodic hypothesis as it relates the ensemble averages to the time averages. This hypothesis implies that the ensemble and time averages are equivalent.

2.4 Hamiltonian dynamics

The basic form of the original formulation of MD follows Hamiltonian dynamics[4]. Using Hamiltonian dynamics, the classical Hamilton's equation of motion[2, 4] shown by equation (2.2.2), can be defined in symplectic form as

$$\dot{x}_i = \sum_{i,j=1}^{2N} \mathcal{B}_{ij} \frac{\partial \mathcal{H}}{\partial x_j}, \tag{2.4.1}$$

where

$$\mathcal{B} = \begin{bmatrix} 0 & 1 \\ -1 & 0 \end{bmatrix}, \tag{2.4.2}$$

is the symplectic matrix in block form and $x = (q, p)$ denotes the phase space point, q and p are the generalized coordinates and momenta, respectively.

The Poisson bracket can be defined as

$$\{a(x), b(x)\} = \sum_{i,j=1}^{2N} \frac{\partial a}{\partial x_i} \mathcal{B}_{ij} \frac{\partial b}{\partial x_j}, \tag{2.4.3}$$

where $a(x)$ and $b(x)$ are arbitrary phase space functions, thus the equations of motion can then be re-written in the form

$$\dot{x}_i = \{x_i, \mathcal{H}\}. \tag{2.4.4}$$

The algebra is called Hamiltonian (or Lie)[4] if the following properties are satisfied by the Poisson bracket[27]

$$\begin{aligned}
\{a, b\} &= -\{b, a\}, & (2.4.5)\\
\{const \times a, b\} &= const \times \{a, b\}, & (2.4.6)\\
\{a + b, c\} &= \{a, c\} + \{b, c\}, & (2.4.7)\\
\{ab, c\} &= a\{b, c\} + \{a, c\} b, & (2.4.8)
\end{aligned}$$

as well as the Jacobi relation

$$\mathcal{J} = \{\{a, b\}, c\} + \{\{c, a\}, b\} + \{\{b, c\}, a\} = 0, \tag{2.4.9}$$

where a, b, c are arbitrary phase space functions. Property (2.4.5) indicates the antisymmetry within the bracket, properties (2.4.6 - 2.4.8) indicates a linear operation within the bracket for elements of $\mathcal{A}$ which can be considered as a space of mathematical objects $\{a, b, c, \ldots\}$ and any complex numbers which are constants, while the fulfillment of property (2.4.9), that is $\mathcal{J} = 0$, indicates that the algebra is left invariant under a time evolution[19].

2.5 Integrating the equations of motion

2.5.1 Introduction

There are various numerical ways in integrating the equations of motion under MD. The main problem faced is in the evaluation of the interacting forces. There is no analytical solution of the potential energy which is a function dependent on the positions of all the particles in the system, hence the forces can only be evaluated numerically as they are computed from the potential energy. Thus a suitable method has to have the following characteristics: it is energy conserving, time reversible, evaluates only one force per time step and is computationally efficient[2]. Among the many numerical methods available (see the following references [1, 21, 25, 27, 28, 29, 30] for other methods), the verlet algorithm [28, 29, 30] is one of widely used method. This particular scheme is a widely implemented time integration algorithm method in MD.

2.5.2 Verlet algorithm

The Verlet algorithm method, which is a third-order Störmer algorithm, was first popularized by Verlet[31] in 1967. The derivation of the algorithm follows from the Taylor expansion about the coordinate variable $x(t)$:

$$x(t+\tau) = x(t) + \dot{x}(t)\tau + \ddot{x}(t)\frac{\tau^2}{2} + \dddot{x}(t)\frac{\tau^3}{6} + \mathcal{O}\left(\tau^4\right)\cdots \tag{2.5.1}$$

$$x(t-\tau) = x(t) - \dot{x}(t)\tau + \ddot{x}(t)\frac{\tau^2}{2} - \dddot{x}(t)\frac{\tau^3}{6} + \mathcal{O}\left(\tau^4\right)\cdots \tag{2.5.2}$$

Summing equations (2.5.1) and (2.5.2)

$$
\begin{aligned}
x(t+\tau)+x(t-\tau) &= 2x(t)+\ddot{x}(t)\tau^2+\mathcal{O}\left(\tau^4\right), \\
x(t+\tau) &= 2x(t)-x(t-\tau)+\ddot{x}(t)\tau^2+\mathcal{O}\left(\tau^4\right). \quad (2.5.3)
\end{aligned}
$$

This Verlet algorithm method uses the positions $x(t)$, accelerations $\ddot{x}(t)$ and positions $x(t-\tau)$ from the previous time step to evaluate new positions at time step $(t+\tau)$. New trajectories are calculated to an error of order τ^4 and without the need of the velocities according to equation (2.5.3). However, the velocities are not essential during the time evolution rather they are needed to evaluate the kinetic energy of the particles. The total energy E of the system can be calculated using the kinetic energy K and the potential energy V according to $E=K+V$. As a result one can test for conservation of the total energy throughout the evolution of the simulation. The velocities can be obtained by subtracting equations (2.5.1) and (2.5.2)

$$
\begin{aligned}
x(t+\tau)-x(t-\tau) &= 2\tau\dot{x}(t), \\
\dot{x}(t) &= \frac{x(t+\tau)-x(t-\tau)}{2\tau}. \quad (2.5.4)
\end{aligned}
$$

The error associated with equation (2.5.4) is of order τ^2. Moreover, one needs to know the coordinate $x(t+\tau)$ in order to evaluate the velocity $\dot{x}(t)$. In order to obtain more accurate values of the velocities and minimize the inconveniences present within equation (2.5.4), more computational resources are required in storing extra variables. Various methods have recently been proposed [1, 3, 25] to overcome the deficiencies already present within the Verlet algorithm. One such proposed method is the velocity Verlet algorithm.

2.5.3 Velocity Verlet algorithm

The velocity Verlet algorithm[32] is derived directly from the Verlet algorithm. New positions at time step $(t+\tau)$ are evaluated using the positions $x(t)$, velocities $\dot{x}(t)$ and accelerations $\ddot{x}(t)$ all at the same time step t. The algorithm is described using the following equations

$$x(t+\tau) = x(t) + \tau\dot{x}(t) + \frac{\tau^2}{2}\ddot{x}(t) \tag{2.5.5}$$

$$\dot{x}(t+\tau) = \dot{x}(t) + \frac{\tau}{2}\left[\ddot{x}(t) + \ddot{x}(t+\tau)\right]. \tag{2.5.6}$$

By eliminating the velocities in the above equations, the Verlet algorithm may be recovered. When performing the integration with the equations of motion, the cycle is implemented using the following steps:

1. Calculate an approximate velocity at mid-step

$$\dot{x}\left(t+\frac{\tau}{2}\right) = \dot{x}(t) + \frac{\tau}{2}\cdot\ddot{x}(t) \tag{2.5.7}$$

2. Calculate position

$$x(t+\tau) = x(t) + \tau\cdot\dot{x}\left(t+\frac{\tau}{2}\right) \tag{2.5.8}$$

3. Calculate acceleration $\ddot{x}(t+\tau)$ from potential energy which is a function of $x(t+\tau)$

4. Calculate velocity at time $t+\tau$

$$\dot{x}(t+\tau) = \dot{x}\left(t+\frac{\tau}{2}\right) + \frac{\tau}{2}\cdot\ddot{x}(t+\tau) \tag{2.5.9}$$

2.6 Molecular dynamics in different ensembles

2.6.1 Introduction

MD simulations study the dynamical evolution of a system with time and are performed at constant energy conditions which correspond to the microcanonical ensemble. Constant energy conditions are difficult to replicate within real life conditions. Real experiments are mostly carried out at constant temperature. In order to compare results from MD with laboratory experiments, the calculations have to be performed in the canonical ensemble. In this section, we give a brief overview of microcanonical and canonical ensembles, and also show how temperature is estimated within MD.

2.6.2 Microcanonical ensemble

This statistical ensemble is characterized by a system having fixed thermodynamical parameters N, V, E which correspond to the number of particles, the volume and the energy respectively. Such a system has an equilibrium distribution function f_m given by

$$f_m(q,p) = Z^{-1}\delta(H-E), \tag{2.6.1}$$

where Z is the partition function given by

$$Z = \int d^N q\, d^N p\, \delta(H-E), \tag{2.6.2}$$

and $\delta(H-E)$ is the delta of Dirac which is characterized as having a zero value except when $H-E=0$, in which case it is infinite. The delta of Dirac function mathematically enforces energy conservation within this ensemble as it ensures $\delta(H-E) \neq 0$ when $H=E$.

Under the principle of equal *a priori* probabilities one can realize that all the microscopic states (q, p) with energy $H = E$ are equally probable. It follows that all the microstates must have the same energy E. However, given E little will be known about the microstates. This inadvertently leads to a system where some of the microstates are preferred and assigned higher probabilities than others. Hence in order to obtain averages in the microcanonical ensemble, all possible microstates have to be considered. This, however, proves to be extremely difficult to evaluate since ensemble averages (see Eq. (2.3.10)) require knowledge of all possible microscopic states. Using the ergodic hypothesis, ensemble averages are equivalent to time averages (see Eq. (2.3.1)) obtained when performing experiments numerically under MD simulation. In reality, experiments are carried out with knowledge of the macroscopic properties such as temperature or pressure. Thus, results from numerical experiments can be compared with real ones if one performs the calculations in the canonical ensemble.

2.6.3 Canonical ensemble

This statistical ensemble is characterized by a system having the macrostates N, V, T which correspond to the number of particles, the volume and the temperature respectively. Temperature control within this ensemble is achieved by placing the system of interest in contact with a heat bath, which in the thermodynamic limit is represented using an infinite number of degrees of freedom. Such a system has an equilibrium distribution function f_c that is dependent on the temperature given by

$$f_c\left(q, p\right) = Z^{-1} e^{-\beta H}, \tag{2.6.3}$$

where Z is the partition function given by

$$Z = \int d^N q \, d^N p \, e^{-\beta H}, \tag{2.6.4}$$

and

$$\beta = \frac{1}{k_B T}, \tag{2.6.5}$$

where k_B is the Boltzmann constant.

Using the canonical distribution function, given by Eq. (2.6.3), one can easily show how to obtain the famous Maxwell distribution function. This function governs the probability distribution of particle velocities in a system in contact with a thermal bath. It also forms the basis for deriving the celebrated Equipartition theorem expressed as

$$\left\langle \frac{p_i^2}{2m_i} \right\rangle = \frac{k_B T}{2}. \tag{2.6.6}$$

Eq. (2.6.6), states that the equilibrium average of the kinetic energy of an arbitrary particle is constant and equal to $k_B T/2$.

2.6.4 Estimating temperature under molecular dynamics

We have seen that at the thermodynamical equilibrium the temperature is related to the ensemble average of the kinetic energy of the particles in the system. Also, we have seen that time averages obtained through MD are equal to the ensemble averages under the ergodic hypothesis.

Temperature, under MD, can be estimated using the equipartition theorem and assuming ergodicity. Hence for a system with N degrees of freedom, the equipartition theorem can be rewritten as

$$\left\langle \sum_{i=1}^{N} \frac{p_i^2}{2m_i} \right\rangle = N \left\langle \frac{p_i^2}{2m_i} \right\rangle = N \frac{k_B T}{2}. \tag{2.6.7}$$

Thus the temperature can be given using the following equation,

$$T = \frac{2}{Nk_B} \left\langle \sum_{i=1}^{N} \frac{p_i^2}{2m_i} \right\rangle . \tag{2.6.8}$$

The instantaneous temperature can also be calculated using

$$T_t = \frac{2}{Nk_B} \sum_{i=1}^{N} \frac{p_i^2}{2m_i}. \tag{2.6.9}$$

The instantaneous temperature times the Boltzmann constant $k_B T_t$ is only an estimate of the inverse of the fixed parameter β of the distribution function which can fluctuate.

Chapter 3

Non-Hamiltonian dynamics

In this chapter, I shall introduce the generalized algebraic bracket used within non-Hamiltonian dynamics and I shall further show how to obtain the compressibility for the following extended systems; Nosé-Hoover, Nosé-Hoover chain and Bulgac-Kusnezov thermostats.

For a very long time, non-Hamiltonian dynamics has been introduced in MD simulations to obtain statistical averages results in various ensembles[6, 7, 10, 33, 34] by using additional thermostats and/or barostats coupled to the system of interest. These additional thermostats together with the physical system of interest make up what is known as the extended system. In the 1980s, Andersen [5] made a significant contribution to the MD computational approach with his work on constant pressure MD using the extended system[10]. By representing the thermal reservoir using additional degrees of freedom one can use the extended system to explore the phase space of a physical system according to a desired ensemble distribution different from the microcanonical distribution function. Moreover, the desired ensemble distribution is found through averaging the extended variables obtained from the physical system as it dynamically explores a hyper surface of constant energy that corresponds

to a microcanonical like distribution function in the extended phase space. Extended systems maintain a well defined conserved energy in the extended phase space.

In Ref.[5], a general mathematical structure has been introduced for conservative non-Hamiltonian equations of motion. Furthermore, it is shown that the conserved dynamical quantity, the "extended energy" simply referred to as the Hamiltonian, is used in specifying the phase space flow. It is also noted that for a given fixed conserved Hamiltonian obtained from a general structure of the equations of motion one can select the compressibility of phase space and obtain an ensemble distribution for the physical system of interest. The compressibility, in non-Hamiltonian dynamics, is deemed as the key in building the invariant measure of phase space [35]. In this chapter we shall introduce the generalized algebraic bracket[15] used within non-Hamiltonian dynamics and show how to obtain the compressibility for the following extended systems; Nosé-Hoover, Nosé-Hoover chain and Bulgac-Kusnezov thermostats.

Consider a conserved time-independent Hamiltonian $\mathcal{H}$, the equations of motion can be written in a general symplectic form

$$\dot{x} = \sum_{j=1}^{2N} \mathcal{B}_{ij} \frac{\partial \mathcal{H}}{\partial x_j}, \qquad i = 1, 2N, \tag{3.0.1}$$

or in bracket form

$$\dot{x}_i = \{x_i, \mathcal{H}\}, \qquad i = 1, \ldots, 2N, \tag{3.0.2}$$

where the point in phase space $x = (q, p)$ is given by the N generalized coordinates q and the N generalized momenta p. $\mathcal{B}_{ij}$ is an antisymmetric matrix

$$\mathcal{B}_{ij} = -\mathcal{B}_{ji}, \qquad i, j = 1, 2N, \tag{3.0.3}$$

which has the same $2N$ dimensions as the phase space and whose elements are a general function of $\mathbf{x}$. This matrix can be written in block form [15, 5] as

$$\mathcal{B} = \begin{bmatrix} 0 & 1 \\ -1 & 0 \end{bmatrix}, \tag{3.0.4}$$

and is used in discussing symplectic properties of canonical transformations. When a noncanonical transformation is applied to the phase space coordinates, the matrix $\mathcal{B}$ loses its canonical form[36] but remains anti-symmetric. Throughout the transformation, equation (3.0.1) preserves the same structure used in the noncanonical Hamiltonian dynamics [36, 37].

Under any phase space flow defined by equation (3.0.2) a time-independent Hamiltonian will be a constant of motion due to the anti-symmetric nature of the matrix $\mathcal{B}_{ij}$. By taking the total time derivative of $\mathcal{H}$, one finds that is essentially taking the trace of the product of a symmetric matrix $\partial\mathcal{H}/\partial x_i \partial\mathcal{H}/\partial x_j$ with an antisymmetric matrix $\mathcal{B}_{ij}$; such a trace is identically zero [5, 15]:

$$\begin{aligned} \frac{d\mathcal{H}}{dt} &= \{\mathcal{H}, \mathcal{H}\}, \\ &= \sum_{i=1}^{2N} \frac{\partial \mathcal{H}}{\partial x_i} \dot{x}_i, \\ &= \sum_{i,j=1}^{2N} \frac{\partial \mathcal{H}}{\partial x_i} \mathcal{B}_{ij} \frac{\partial \mathcal{H}}{\partial x_j} = 0. \end{aligned} \tag{3.0.5}$$

It is interesting to note that the property shown in equation (3.0.5) is always valid for flows described by equation (3.0.1) provided that the matrix $\mathcal{B}_{ij}$ is antisymmetric in nature. This has been exploited by Sergi and Ferrario[5] for introducing and defining non-Hamiltonian conservative phase space flows[15].

Since the bracket in equation (3.0.2) remains conserved under noncanonical

transformations, it is used in defining expressions for non-Hamiltonian phase space flows. However, it must be pointed out that it does not satisfy the Jacobi relation which is an important algebraic property. As seen from the previous chapter, the properties satisfied within Hamiltonian dynamics by the Poisson bracket[27] are

$$\begin{aligned} \{a,b\} &= -\{b,a\}, & (3.0.6)\\ \{const \times a,b\} &= const \times \{a,b\}, & (3.0.7)\\ \{a+b,c\} &= \{a,c\}+\{b,c\}, & (3.0.8)\\ \{ab,c\} &= a\{b,c\}+\{a,c\}b, & (3.0.9) \end{aligned}$$

and the Jacobi relation

$$\mathcal{J} = \{\{a,b\},c\}+\{\{c,a\},b\}+\{\{b,c\},a\} = 0, \qquad (3.0.10)$$

where a, b, c are arbitrary phase space functions. If the matrix $\mathcal{B}_{ij}$ holds in equation (3.0.4) and satisfies the following condition

$$\sum_{n=1}^{2N}\left(\mathcal{B}_{in}\frac{\partial \mathcal{B}_{jk}}{\partial x_n}+\mathcal{B}_{kn}\frac{\partial \mathcal{B}_{ij}}{\partial x_n}+\mathcal{B}_{jn}\frac{\partial \mathcal{B}_{ki}}{\partial x_n}\right) = 0, \qquad (3.0.11)$$

for any index i, j, k then the flux in phase space remains Hamiltonian. Thus, as a basis of determining noncanonical Hamiltonian flows [36, 37], Eq. (3.0.1) is used provided that the conditions described by Eqs. (3.0.3) and (3.0.11) are satisfied. One such example of the noncanonical Hamiltonian dynamics is the Andersen constant pressure equations of motion[10].

For non-Hamiltonian dynamics, all the other properties shown in Eqs. (3.0.6-3.0.9) hold with the exception of the Jacobi relation, that is $\mathcal{J} \neq 0$. The failure

of the Jacobi implies that the algebra lacks invariance under time translations. In order to illustrate this feature, lets consider the Jacobi relation $\mathcal{J}$ [15],

$$\{a,\{b,\mathcal{H}\}\}+\{\mathcal{H}\{a,b\}\}+\{b,\{\mathcal{H},a\}\}=\mathcal{J}, \tag{3.0.12}$$

where a, b are the phase space variables and $\mathcal{H}$ is the Hamiltonian. Performing a direct calculation, one can show that

$$\mathcal{J}=\sum_{i,j,k,n}\frac{\partial a}{\partial x_i}\frac{\partial b}{\partial x_j}\frac{\partial \mathcal{H}}{\partial x_k}\left(\mathcal{B}_{in}\frac{\partial \mathcal{B}_{jk}}{\partial x_n}+\mathcal{B}_{kn}\frac{\partial \mathcal{B}_{ij}}{\partial x_n}+\mathcal{B}_{jn}\frac{\partial \mathcal{B}_{ki}}{\partial x_n}\right). \tag{3.0.13}$$

From the above equation one gets

$$\{\{a,b\},\mathcal{H}\}=\{\dot{a},b\}+\left\{a,\dot{b}\right\}+\mathcal{J}, \tag{3.0.14}$$

which can be written as

$$\frac{d}{dt}\{a,b\}=\{\dot{a},b\}+\left\{a,\dot{b}\right\}+\mathcal{J}. \tag{3.0.15}$$

An important feature emerges from Eq. (3.0.15). The equation shows that under time translation the non-Hamiltonian algebra lack invariance. Thus, non-Hamiltonian bracket of two constants of motion is no longer a constant of motion because of a non-zero Jacobi relation.

The equations of motion defined by Eq. (3.0.1) will generally lead to a non-zero phase space compressibility being defined. The compressibility can be derived as follows,

$$\begin{aligned}\kappa(x) &= \sum_{i}^{2N} \frac{\partial \dot{x}_i}{\partial x_i}, \\ &= \sum_{i,j}^{2N} \frac{\partial}{\partial x_i}\left(\mathcal{B}_{ij}\frac{\partial \mathcal{H}}{\partial x_j}\right), \\ &= \sum_{i,j}^{2N} \left(\frac{\partial \mathcal{B}_{ij}}{\partial x_i}\frac{\partial \mathcal{H}}{\partial x_j} + \mathcal{B}_{ij}\frac{\partial^2 \mathcal{H}}{\partial x_j x_i}\right), \end{aligned} \tag{3.0.16}$$

where the second term in Eq. (3.0.16) is identically zero since it is the product of a symmetric matrix with the trace of an antisymmetric one $\mathcal{B}_{ij}$. Thus, the compressibility is

$$\kappa(x) = \sum_{i,j}^{2N} \frac{\partial \mathcal{B}_{ij}}{\partial x_i}\frac{\partial \mathcal{H}}{\partial x_j}. \tag{3.0.17}$$

Having a non-zero phase space compressibility means that the dynamics will not sample the phase space uniformly. However, the approach proposed in Ref. [35] exploits the ergodic hypothesis to determine explicitly the corresponding weight in phase space. By choosing the form of the conserved Hamiltonian $\mathcal{H}$, we can construct particular phase space compressibility κ. This is made possible by exploiting the structure of Eq. (3.0.1) as it allows one the freedom to choose the matrix elements $\mathcal{B}_{ij}$ [5]. As a result, conservative non-Hamiltonian equations of motion can be derived with a controlled statistical weight of the phase space. Such an approach may lead to other possibilities of formulating non-Hamiltonian dynamics with statistical constraints. In order to address the general features of non-Hamiltonian dynamics, only static equilibrium properties shall be discussed within this thesis. This restriction will, in turn, help when designing ergodic systems.

3.1 Extended system dynamics

In MD simulations, the underlined structure found in Eq. (3.0.1) exists for nearly all, if not most of the equations of motion for the extended systems. In this section we show how to obtain the compressibility for the following deterministic thermostats; Nosé-Hoover, Nosé-Hoover chain and Bulgac-Kusnezov thermostats.

3.1.1 Nosé-Hoover thermostat

The dynamics for a one-dimensional system that is coupled to a Nosé-Hoover thermostat has a $2N+2$ dimensional phase space where the phase space points are denoted by $x = (q, \eta, p, p_\eta)$. The Nosé-Hoover Hamiltonian is

$$\mathcal{H}^{NH} = \sum_{i=1}^{N} \frac{p_i^2}{2m_i} + V(q) + \frac{p_\eta^2}{2m_\eta} + Nk_BT\eta, \tag{3.1.1}$$

where (q, p) are the coordinates and momenta respectively. m is the oscillator mass, while η is the thermostat variable with the corresponding fictitious mass m_η with its associated momenta p_η. k_B is the Boltzmann constant whereas T is the temperature.

The equations of motion are given by[34]

$$\dot{q}_i = \frac{p_i}{m_i}, \tag{3.1.2}$$

$$\dot{p}_i = F_i - \frac{p_\eta}{m_\eta} p_i, \tag{3.1.3}$$

$$\dot{\eta} = \frac{p_\eta}{m_\eta}, \tag{3.1.4}$$

$$\dot{p}_\eta = \sum_{i=1}^{N} \frac{p_i^2}{m_i} - Nk_BT. \tag{3.1.5}$$

Equations (3.1.2-3.1.5) can be re-written in matrix form by using Eq. (3.0.1) and evaluating explicitly $\partial\mathcal{H}/\partial x$ one can find the anti-symmetric matrix $\mathcal{B}_{NH}$. The tensorial form of equations (3.1.2-3.1.5) is (in block form)

$$\begin{bmatrix} \dot{q}_i \\ \dot{\eta} \\ \dot{p}_i \\ \dot{p}_\eta \end{bmatrix} = \begin{bmatrix} 0 & 0 & 1 & 0 \\ 0 & 0 & 0 & 1 \\ -1 & 0 & 0 & -p_i \\ 0 & -1 & p_i & 0 \end{bmatrix} \begin{bmatrix} -F_i \\ Nk_BT \\ \frac{p_i}{m_i} \\ \frac{p_\eta}{M_\eta} \end{bmatrix}, \tag{3.1.6}$$

where the anti-symmetric matrix is,

$$\mathcal{B}_{NH} = \begin{bmatrix} 0 & 0 & 1 & 0 \\ 0 & 0 & 0 & 1 \\ -1 & 0 & 0 & -p_i \\ 0 & -1 & p_i & 0 \end{bmatrix}. \tag{3.1.7}$$

Equation (3.1.6) shows the phase space flow given in Eq. (3.0.1) is conserved and satisfies the structure of non-Hamiltonian dynamics given by Nosé-Hoover equations of motion[5].

Using equation (3.0.17), one can find the compressibility of the Nosé-Hoover thermostat as follows

$$\kappa = \sum_{i,j}^{2N} \frac{\partial \mathcal{B}_{ij}^{NH}}{\partial x_i} \frac{\partial \mathcal{H}_{NH}}{\partial x_j}, \tag{3.1.8}$$

$$= -\frac{p_\eta}{m_\eta}. \tag{3.1.9}$$

Upon introducing the extended phase space function

$$\mathcal{H}_T^{NH} = \mathcal{H} + \frac{p_\eta^2}{2m_\eta}, \tag{3.1.10}$$

and taking a total time derivative of Eq. (3.1.10) and using the equations of motion, one finds

$$\frac{d\mathcal{H}_T^{NH}}{dt} = -Nk_BT\frac{p_\eta}{m_\eta}, \tag{3.1.11}$$

which can be related to the compressibility by

$$\kappa = -\frac{p_\eta}{m_\eta} = \beta\frac{d\mathcal{H}_T^{NH}}{dt}, \tag{3.1.12}$$

where $\beta = 1/k_BT$.

A derivation for the associated invariant measure of the Nosé-Hoover thermostat has been shown in Appendix B.1.

3.1.2 Nosé-Hoover chain thermostat

The dynamics for a one-dimensional system that is coupled to a Nosé-Hoover Chain thermostat has a $2N + 4$ dimensional phase space where the phase space points are denoted by $x = (q, \eta_1, \eta_2, p, p_{\eta_1}, p_{\eta_2})$. The Nosé Hoover chain Hamiltonian is

$$\mathcal{H}^{NHC} = \sum_{i=1}^{N}\frac{p_i^2}{2m_i} + V(q) + \frac{p_{\eta_1}^2}{2m_{\eta_1}} + \frac{p_{\eta_2}^2}{2m_{\eta_2}} + Nk_BT\eta_1 + k_BT\eta_2, \tag{3.1.13}$$

where (q, p) are the $2N$ coordinates and momenta respectively. m is the oscillator mass, while η_1 and η_2 are the two thermostat variables with the cor-

responding fictitious masses m_{η_1} and m_{η_2}, and their associated momenta p_{η_1} and p_{η_2}. k_B is the Boltzmann constant whereas T is the temperature.

The equations of motion are given by [34]

$$\dot{q}_i = \frac{p_i}{m_i}, \tag{3.1.14}$$

$$\dot{\eta}_1 = \frac{p_{\eta_1}}{m_{\eta_1}}, \tag{3.1.15}$$

$$\dot{\eta}_2 = \frac{p_{\eta_2}}{m_{\eta_2}}, \tag{3.1.16}$$

$$\dot{p}_i = -\frac{\partial V(q)}{\partial q_i} - p_i \frac{p_{\eta_1}}{m_{\eta_1}}, \tag{3.1.17}$$

$$\dot{p}_{\eta_1} = \sum_{i=1}^{N} \left(\frac{p_i^2}{m_i} - k_B T \right) - p_{\eta_1} \frac{p_{\eta_2}}{m_{\eta_2}}, \tag{3.1.18}$$

$$\dot{p}_{\eta_2} = \frac{p_{\eta_1}^2}{m_{\eta_1}} - k_B T. \tag{3.1.19}$$

Equations (3.1.14-3.1.19) can be re-written in matrix form by using Eq. (3.0.1) and evaluating explicitly $\partial \mathcal{H}/\partial x$ one can find the anti-symmetric matrix $\mathcal{B}_{NH}$. The tensorial form of Eqs. (3.1.14-3.1.19) is (in block form)

$$\begin{bmatrix} \dot{q}_i \\ \dot{\eta} \\ \dot{\chi} \\ \dot{p}_i \\ \dot{p}_{\eta_1} \\ \dot{p}_{\eta_2} \end{bmatrix} = \begin{bmatrix} 0 & 0 & 0 & 1 & 0 & 0 \\ 0 & 0 & 0 & 0 & 1 & 0 \\ 0 & 0 & 0 & 0 & 0 & 1 \\ -1 & 0 & 0 & 0 & -p_i & 0 \\ 0 & -1 & 0 & p_i & 0 & -p_{\eta_1} \\ 0 & 0 & -1 & 0 & p_{\eta_1} & 0 \end{bmatrix} \begin{bmatrix} -F_i(q) \\ N k_B T \\ k_B T \\ \frac{p_i}{m_i} \\ \frac{p_{\eta_1}}{M_{\eta_1}} \\ \frac{p_{\eta_2}}{M_{\eta_2}} \end{bmatrix}, \tag{3.1.20}$$

where the anti-symmetric matrix is,

$$\mathcal{B}_{NHC} = \begin{bmatrix} 0 & 0 & 0 & 1 & 0 & 0 \\ 0 & 0 & 0 & 0 & 1 & 0 \\ 0 & 0 & 0 & 0 & 0 & 1 \\ -1 & 0 & 0 & 0 & -p_i & 0 \\ 0 & -1 & 0 & p_i & 0 & -p_{\eta_1} \\ 0 & 0 & -1 & 0 & p_{\eta_1} & 0 \end{bmatrix}. \tag{3.1.21}$$

Equation (3.1.20) shows the phase space flow given in Eq. (3.0.1) is conserved and satisfies the structure of non-Hamiltonian dynamics given by Nosé-Hoover chain equations of motion[5].

Using equation (3.0.17), one can find the compressibility of the Nosé-Hoover chain thermostat as follows

$$\kappa = \sum_{i,j=1}^{2N} \frac{\partial \mathcal{B}_{ij}^{NHC}}{\partial x_i} \frac{\partial \mathcal{H}_{NHC}}{\partial x_j}, \tag{3.1.22}$$

$$= -\frac{p_{\eta_1}}{m_{\eta_1}} - \frac{p_{\eta_2}}{m_{\eta_2}}, \tag{3.1.23}$$

upon introducing the extended phase space function:

$$\mathcal{H}_T^{NHC} = \mathcal{H} + \frac{p_{\eta_1}^2}{2m_{\eta_1}} + \frac{p_{\eta_2}^2}{2m_{\eta_2}}, \tag{3.1.24}$$

taking a total time derivative of Eq. (3.1.24) and using the equations of motion, one finds

$$\frac{d\mathcal{H}_T^{NHC}}{dt} = k_B T \left(-\frac{p_{\eta_1}}{m_{\eta_1}} - \frac{p_{\eta_2}}{m_{\eta_2}} \right), \tag{3.1.25}$$

which can be related to the compressibility by

$$\kappa = -\frac{p_{\eta_1}}{m_{\eta_1}} - \frac{p_{\eta_2}}{m_{\eta_2}} = \beta \frac{d\mathcal{H}_T^{NHC}}{dt}, \tag{3.1.26}$$

where $\beta = 1/k_B T$.

A derivation for the associated invariant measure of the Nosé-Hoover chain thermostat has been shown in Appendix B.2.

3.1.3 Bulgac-Kusnezov thermostat

The dynamics for a one-dimensional system that is coupled to a Bulgac-Kusnezov thermostat has a $2N + 4$ dimensional phase space where the phase space points are denoted by $x = (q, \zeta, \xi, p, p_\zeta, p_\xi)$[14, 38, 39, 40]. The Hamiltonian of the system is given as

$$\mathcal{H}^{BK} = \sum_{i=1}^{N} \frac{p_i^2}{2m_i} + V(q) + \frac{p_\zeta^2}{2m_\zeta} + \frac{p_\xi^2}{2m_\xi} + N k_B T \zeta + N k_B T \xi, \tag{3.1.27}$$

where (q, p) are the coordinates and momenta respectively. m is the oscillator mass, while ζ and ξ are the Bulgac-Kusnezov 'demons' with the corresponding fictitious masses m_ζ and m_ξ, and their associated momenta p_ζ and p_ξ. k_B is the Boltzmann constant whereas T is the temperature.

The equations of motion are given by

$$\dot{q}_i = \frac{p_i}{m_i} - q_i \frac{p_\xi}{m_\xi}, \tag{3.1.28}$$

$$\dot{\zeta} = \frac{p_\zeta}{m_\zeta}, \tag{3.1.29}$$

$$\dot{\xi} = \frac{p_\xi}{m_\xi}, \tag{3.1.30}$$

$$\dot{p}_i = F_i - p_i \frac{p_\zeta}{m_\zeta}, \tag{3.1.31}$$

$$\dot{p}_\zeta = \sum_{i=1}^{N} \left(\frac{p_i^2}{m_i} - k_B T \right), \tag{3.1.32}$$

$$\dot{p}_\xi = -\sum_{i=1}^{N} \left(q_i F_i + k_B T \right). \tag{3.1.33}$$

Equations (3.1.28-3.1.33) can be re-written in matrix form by using Eq. (3.0.1) and evaluating explicitly $\partial \mathcal{H}/\partial x$ one can find the anti-symmetric matrix $\mathcal{B}_{BK}$. The tensorial form of Eqs. (3.1.28-3.1.33) is

$$\begin{bmatrix} \dot{q}_i \\ \dot{\zeta} \\ \dot{\xi} \\ \dot{p}_i \\ \dot{p}_\zeta \\ \dot{p}_\xi \end{bmatrix} = \begin{bmatrix} 0 & 0 & 0 & 1 & 0 & -q_i \\ 0 & 0 & 0 & 0 & 1 & 0 \\ 0 & 0 & 0 & 0 & 0 & 1 \\ -1 & 0 & 0 & 0 & -p_i & 0 \\ 0 & -1 & 0 & p_i & 0 & 0 \\ q_i & 0 & -1 & 0 & 0 & 0 \end{bmatrix} \begin{bmatrix} -F_i(q) \\ N k_B T \\ N k_B T \\ \frac{p_i}{m_i} \\ \frac{p_\zeta}{M_\zeta} \\ \frac{p_\xi}{M_\xi} \end{bmatrix}, \tag{3.1.34}$$

where the anti-symmetric matrix is,

$$\mathcal{B}^{BK} = \begin{bmatrix} 0 & 0 & 0 & 1 & 0 & -q_i \\ 0 & 0 & 0 & 0 & 1 & 0 \\ 0 & 0 & 0 & 0 & 0 & 1 \\ -1 & 0 & 0 & 0 & -p_i & 0 \\ 0 & -1 & 0 & p_i & 0 & 0 \\ q_i & 0 & -1 & 0 & 0 & 0 \end{bmatrix}. \tag{3.1.35}$$

Equation (3.1.20) shows the phase space flow given in Eq. (3.0.1) is conserved and satisfies the structure of non-Hamiltonian dynamics given by Nosé-Hoover chain equations of motion[5].

Using equation (3.0.17), one can find the compressibility of the Bulgac-Kusnezov thermostat as follows

$$\kappa = \sum_{i,j=1}^{2N} \frac{\partial \mathcal{B}_{ij}^{BK}}{\partial x_i} \frac{\partial \mathcal{H}_{BK}}{\partial x_j}, \tag{3.1.36}$$

$$= -\frac{p_\zeta}{m_\zeta} - \frac{p_\xi}{m_\xi}, \tag{3.1.37}$$

upon introducing the extended phase space function:

$$\mathcal{H}_T^{BK} = \mathcal{H} + \frac{p_\zeta^2}{2m_\zeta} + \frac{p_\xi^2}{2m_\xi}, \tag{3.1.38}$$

taking a total time derivative of Eq. (3.1.38) and using the equations of motion, one finds

$$\frac{d\mathcal{H}_T^{BK}}{dt} = k_B T \left(-\frac{p_\zeta}{m_\zeta} - \frac{p_\xi}{m_\xi} \right), \tag{3.1.39}$$

which can be related to the compressibility by

$$\kappa = -\frac{p_\zeta}{m_\zeta} - \frac{p_\xi}{m_\xi} = \beta \frac{d\mathcal{H}_T^{BK}}{dt}, \tag{3.1.40}$$

where $\beta = 1/k_B T$.

A derivation for the associated invariant measure of the Bulgac-Kusnezov thermostat has been shown in Appendix B.3.

Chapter 4

Time-reversible and measure-preserving algorithms

In this chapter, I show how to derive systematically time-reversible and measure-preserving algorithms for the following deterministic thermostats; Nosé-Hoover, Nosé-Hoover Chain and Bulgac-Kusnezov thermostats.

4.1 Time-reversible algorithms

In the previous chapter, the concept of non-Hamiltonian dynamics has been defined and justified. One is now faced with searching for appropriate algorithms for integrating non-Hamiltonian equations of motion. The numerical algorithm to be derived is one that is conjured up by renouncing some basic theoretical properties (such as time-invariance of the bracket algebra) and has to be such that it does not break any other symmetries of the problem. As mentioned in the work of Sergi [15], in the aforementioned numerical algorithm, the main property that has to be left unchanged is the time-reversal invariance of the phase space trajectory.

Tuckerman *et al* [34] have recently shown how to systematically derive time-reversible algorithms from the Liouville formulation of classical mechanics. Their approach involves the following, starting off with the Trotter expansion of the classical Liouville propagator and the reversible Trotter expansion, several new integrators are derived for solving Newton's equations of motion[1].

Consider an arbitrary function $f\left(p\left(t\right),q\left(t\right)\right)$ with implicit time dependence that depends on all the coordinates q and momenta p of the system. If a time derivative of this function is taken, then $\dot{f}$ will be given by

$$\begin{aligned} \dot{f} &= \dot{q}\frac{\partial f}{\partial q}+\dot{p}\frac{\partial f}{\partial p}, \\ &\equiv iLf, \end{aligned} \tag{4.1.1}$$

where the Liouville operator is defined by

$$iL=\dot{q}\frac{\partial}{\partial q}+\dot{p}\frac{\partial}{\partial p}. \tag{4.1.2}$$

The classical propagator is then

$$U\left(t\right)=e^{iLt}, \tag{4.1.3}$$

which is a unitary operator; that is, $U\left(-t\right)=U^{-1}\left(t\right)$.

The state of the system at time t is given by integrating equation (4.1.1) under which the following formal solution is obtained

$$f\left(p\left(t\right),q\left(t\right)\right)=U\left(t\right)f\left(p\left(0\right),q\left(0\right)\right). \tag{4.1.4}$$

In all cases of practical interest, much cannot be done with this formal solution, because the exact integration of the classical equations of motion are equivalent to evaluating the right-hand side of the equation. However, in a few simple cases the formal solution is known explicitly. In particular, suppose that our Liouville operator (4.1.2) can be decomposed into two parts such that

$$iL = iL_q + iL_p. \tag{4.1.5}$$

Now taking only the first term on the right-hand side of Eq. (4.1.2).

$$iL_q = \dot{q}(0)\frac{\partial}{\partial q}, \tag{4.1.6}$$

where $\dot{q}(0)$ is the initial value of $\dot{q}$ at time $t = 0$. Substituting Eq. (4.1.6) into Eq. (4.1.4) and using a Taylor series expansion of the exponential on the right-hand side, we get

$$\begin{aligned} f(t) &= f(0) + iL_q t f(0) + \frac{(iL_q t)^2}{2!} f(0) + \cdots, \\ &= exp\left(\dot{q}(0)\, t \frac{\partial}{\partial q}\right) f(0), \\ &= \sum_{n=0}^{\infty} \frac{(\dot{q}(0))^n}{n!} \frac{\partial^n}{\partial q^n} f(0), \\ &= f\left[p(0), (q + \dot{q}(0)\, t)\right]. \end{aligned} \tag{4.1.7}$$

From the above result, it can be seen that the effect of $exp(iL_q t)$ is a simple shift of coordinates. Similarly, the effect of $exp(iL_p t)$, with iL_p defined as

$$iL_p = \dot{p}(0)\frac{\partial}{\partial p}, \tag{4.1.8}$$

is a simple shift of momenta.

From Eq. (4.1.5), the total Liouville operator, iL, is equal $iL_q + iL_p$. However, $exp\left(iLt\right) = exp\left(i\left(L_q + L_p\right)t\right)$ is not equivalent to $exp\left(iL_q t\right) \times exp\left(iL_p t\right)$, because iL_q and iL_p are non-commuting operators. Thus using the Trotter theorem one can define $exp\left(i\left(L_q + L_p\right)t\right)$ as follows

$$\begin{aligned} e^{i(L_q+L_p)t} &= \left[e^{i(L_q+L_p)t/P}\right]^P, & (4.1.9)\\ &= \left[e^{iL_q(\triangle t/2)}e^{iL_p\triangle t}e^{iL_q(\triangle t/2)}\right]^P + \mathcal{O}\left(t^3/P^2\right), & (4.1.10)\end{aligned}$$

where $\triangle t = t/P$. From the above, we obtain the following discretized time propagator

$$\begin{aligned} G\left(\triangle t\right) &= U_q\left(\frac{\triangle t}{2}\right)U_p\left(\triangle t\right)U_q\left(\frac{\triangle t}{2}\right), & (4.1.11)\\ &= e^{iL_q(\triangle t/2)}e^{iL_p\triangle t}e^{iL_q(\triangle t/2)}, & (4.1.12)\end{aligned}$$

which is unitary. This property can easily be shown to be the case since the individual operators that compose $G\left(\triangle t\right)$ are separately unitary, therefore $G^{-1}\left(t\right) = G^{\dagger}\left(t\right) = G\left(-t\right)$. The implication of this is that any integrator based on such a Trotter factorization will be reversible[1].

In order to see what the effect is of this operator on the coordinates and momenta of the particles. Let us define

$$f_q\left[\triangle t; f\left(0\right)\right] = U_q\left(\triangle t\right)f\left(0\right) \tag{4.1.13}$$

and

$$f_p\left[\triangle t; f\left(0\right)\right] = U_p\left(\triangle t\right)f\left(0\right) \tag{4.1.14}$$

to be, respectively, the state at time$\triangle t$ when the system is propagated by $U_q(\triangle t)$ or $U_p(\triangle t)$ starting from the state $f(0)$ at time $t = 0$. Applying the operators in equation (4.1.12) serially, that is, first starting off by applying $e^{iL_q(\triangle t/2)}$ to $f(0)$, we obtain

$$\begin{aligned} f(p(\triangle t), q(\triangle t)) &= U_q\left(\frac{\triangle t}{2}\right) U_p(\triangle t)\, U_q\left(\frac{\triangle t}{2}\right) f(p(0), q(0)), \\ &= U_q\left(\frac{\triangle t}{2}\right) U_p(\triangle t)\, f_q\left(\frac{\triangle t}{2}; f(p(0), q(0))\right), \\ &= U_q\left(\frac{\triangle t}{2}\right) f_p\left(\triangle t; f_q\left(\frac{\triangle t}{2}; f(p(0), q(0))\right)\right), \\ &= f_q\left(\frac{\triangle t}{2}; f_p\left(\triangle t; f_q\left(\frac{\triangle t}{2}; f(p(0), q(0))\right)\right)\right). \end{aligned} \tag{4.1.15}$$

Using as an example the formulation of deterministic thermostats by means of non-Hamiltonian dynamics, we can show how in practice a time-reversible algorithm is built. The use of such deterministic thermostats is a culmination of a journey from Boltzmann to Gibbs and then back to Boltzmann as they generally sample the canonical distribution function of a system coupled to a deterministic bath, represented by a few additional degrees of freedom. Examples of such deterministic thermostats are Nosé-Hoover, Nosé-Hoover chain and Bulgac-Kusnezov. In the next sections we shall illustrate the derivation of time-reversible integration algorithms for the Nosé-Hoover, Nosé-Hoover chain and Bulgac-Kusnezov dynamics.

4.1.1 Time-reversible integration of Nosé-Hoover dynamics

The Hamiltonian of Nosé-Hoover dynamics is given by

$$\mathcal{H}^{NH} = \sum_{i=1}^{N} \frac{p_i^2}{2m_i} + V(q) + \frac{p_\eta^2}{2m_\eta} + Nk_BT\eta, \tag{4.1.16}$$

where (q, p) are the coordinates and momenta respectively. m is the oscillator mass, while η is the thermostat variable with the corresponding fictitious mass m_η with its associated momenta p_η. k_B is the Boltzmann constant whereas T is the temperature.

The equations of motion can be defined as

$$\dot{q}_i = \frac{p_i}{m_i}, \tag{4.1.17}$$

$$\dot{p}_i = F_i - \frac{p_\eta}{m_\eta} p_i, \tag{4.1.18}$$

$$\dot{\eta} = \frac{p_\eta}{m_\eta}, \tag{4.1.19}$$

$$\dot{p}_\eta = \sum_{i=1}^{N} \left(\frac{p_i^2}{m_i} - k_BT \right). \tag{4.1.20}$$

The Liouville operator $\mathcal{L}$ is associated with the equations of motion Eqs. (4.1.17) - (4.1.20), and split as

$$\mathcal{L} = \sum_{\alpha=1}^{5} \mathcal{L}_\alpha, \tag{4.1.21}$$

where the single terms are given as follows

$$\mathcal{L}_1 = \sum_{i=1}^{N} \frac{p_i}{m_i} \frac{\partial}{\partial q_i}, \tag{4.1.22}$$

$$\mathcal{L}_2 = \sum_{i=1}^{N} F_i(q) \frac{\partial}{\partial p_i}, \tag{4.1.23}$$

$$\mathcal{L}_3 = -\sum_{i=1}^{N} p_i \frac{p_\eta}{m_\eta} \frac{\partial}{\partial p_i}, \tag{4.1.24}$$

$$\mathcal{L}_4 = \frac{p_\eta}{m_\eta} \frac{\partial}{\partial \eta}, \tag{4.1.25}$$

$$\mathcal{L}_5 = F_{p_\eta} \frac{\partial}{\partial p_\eta}, \tag{4.1.26}$$

where we have defined the following

$$F_i(q) = -\frac{\partial V(q)}{\partial q_i}, \tag{4.1.27}$$

$$F_{p_\eta} = \sum_{i=1}^{N} \left(\frac{p_i^2}{m_i} - k_B T \right). \tag{4.1.28}$$

A propagator

$$U_\alpha(\tau) = exp\left[\tau \mathcal{L}_\alpha\right], \tag{4.1.29}$$

for $\alpha = 1, \ldots, 5$ is associated with each Liouville piece. The Nosé-Hoover propagator can be written explicitly using the symmetric Trotter formula as follows

$$\begin{aligned} U(\tau) &= U_5\left(\frac{\tau}{2}\right) U_4\left(\frac{\tau}{2}\right) U_3\left(\frac{\tau}{2}\right) U_2\left(\frac{\tau}{2}\right), \\ &\times U_1(\tau) U_2\left(\frac{\tau}{2}\right) U_3\left(\frac{\tau}{2}\right) U_4\left(\frac{\tau}{2}\right) U_5\left(\frac{\tau}{2}\right). \end{aligned} \tag{4.1.30}$$

Using the direct translation technique, the pseudo-code form of the time-reversible algorithm is:

$$p_\eta \rightarrow p_\eta + \tfrac{\tau}{2} F_{p_\eta} \Big\} : U_5\left(\tfrac{\tau}{2}\right)$$

$$\left.\begin{array}{rcl} \eta & \rightarrow & \eta + \frac{\tau}{2}\frac{p_\eta}{m_\eta} \end{array}\right\} : U_4\left(\tfrac{\tau}{2}\right)$$

$$\left.\begin{array}{rcl} p_i & \rightarrow & p_i \cdot exp\left[-\frac{\tau}{2}\frac{p_\eta}{m_\eta}\right] \end{array}\right\} : U_3\left(\tfrac{\tau}{2}\right)$$

$$\left.\begin{array}{rcl} p_i & \rightarrow & p_i + \frac{\tau}{2} F_i(q) \end{array}\right\} : U_2\left(\tfrac{\tau}{2}\right)$$

$$\left.\begin{array}{rcl} q_i & \rightarrow & q_i + \tau\frac{p_i}{m_i} \end{array}\right\} : U_1(\tau)$$

$$\left.\begin{array}{rcl} p_i & \rightarrow & p_i + \frac{\tau}{2} F_i(q) \end{array}\right\} : U_2\left(\tfrac{\tau}{2}\right)$$

$$\left.\begin{array}{rcl} p_i & \rightarrow & p_i \cdot exp\left[-\frac{\tau}{2}\frac{p_\eta}{m_\eta}\right] \end{array}\right\} : U_3\left(\tfrac{\tau}{2}\right)$$

$$\left.\begin{array}{rcl} \eta & \rightarrow & \eta + \frac{\tau}{2}\frac{p_\eta}{m_\eta} \end{array}\right\} : U_4\left(\tfrac{\tau}{2}\right)$$

$$p_\eta \rightarrow p_\eta + \tfrac{\tau}{2} F_{p_\eta} \Big\} : U_5\left(\tfrac{\tau}{2}\right)$$

4.1.2 Time-reversible integration of Nosé-Hoover chain dynamics

The Hamiltonian of Nosé-Hoover chain dynamics is given by

$$\mathcal{H}^{NHC} = \sum_{i=1}^{N} \frac{p_i^2}{2m_i} + V(q) + \frac{p_{\eta_1}^2}{2m_{\eta_1}} + \frac{p_{\eta_2}^2}{2m_{\eta_2}} + Nk_BT\eta_1 + k_BT\eta_2, \quad (4.1.31)$$

where (q, p) are the coordinates and momenta respectively. m is the oscillator mass, while η_1 and η_2 are the two thermostat variables with the corresponding fictitious masses m_{η_1} and m_{η_2}, and their associated momenta p_{η_1} and p_{η_2}. k_B is the Boltzmann constant whereas T is the temperature.

The equations of motion are given by

$$\dot{q}_i = \frac{p_i}{m_i}, \tag{4.1.32}$$

$$\dot{\eta}_1 = \frac{p_{\eta_1}}{m_{\eta_1}}, \tag{4.1.33}$$

$$\dot{\eta}_2 = \frac{p_{\eta_2}}{m_{\eta_2}}, \tag{4.1.34}$$

$$\dot{p}_i = -\frac{\partial V(q)}{\partial q_i} - p_i \frac{p_{\eta_1}}{m_{\eta_1}}, \tag{4.1.35}$$

$$\dot{p}_{\eta_1} = \sum_{i=1}^{N} \left(\frac{p_i^2}{m_i} - k_B T \right) - p_{\eta_1} \frac{p_{\eta_2}}{m_{\eta_2}}, \tag{4.1.36}$$

$$\dot{p}_{\eta_2} = \frac{p_{\eta_1}^2}{m_{\eta_1}} - k_B T. \tag{4.1.37}$$

The Liouville operator $\mathcal{L}$ is associated with the equations of motion Eqs. (4.1.32) - (4.1.37), and split as

$$\mathcal{L} = \sum_{\alpha=1}^{5} \mathcal{L}_\alpha, \tag{4.1.38}$$

where the single terms are given as follows

$$\mathcal{L}_1 = \sum_{i=1}^{N} \frac{p_i}{m} \frac{\partial}{\partial q_i} + \frac{p_{\eta_1}}{m_{\eta_1}} \frac{\partial}{\partial \eta_1} + \frac{p_{\eta_2}}{m_{\eta_2}} \frac{\partial}{\partial \eta_2}, \tag{4.1.39}$$

$$\mathcal{L}_2 = \sum_{i=1}^{N} F_i(q) \frac{\partial}{\partial p_i}, \tag{4.1.40}$$

$$\mathcal{L}_3 = -\sum_{i=1}^{N} \frac{p_{\eta_1}}{m_{\eta_1}} p_i \frac{\partial}{\partial p_i}, \tag{4.1.41}$$

$$\mathcal{L}_4 = \left[-\frac{p_{\eta_2}}{m_{\eta_2}} p_{\eta_1} + F_{p_{\eta_1}} \right] \frac{\partial}{\partial p_{\eta_1}}, \tag{4.1.42}$$

$$\mathcal{L}_5 = F_{p_{\eta_2}} \frac{\partial}{\partial p_{\eta_2}}, \tag{4.1.43}$$

where we have defined the following

$$F_i(q) = -\frac{\partial V(q)}{\partial q_i}, \tag{4.1.44}$$

$$F_{p_{\eta_1}} = \sum_{i=1}^{N} \left(\frac{p_i^2}{m} - k_B T \right), \tag{4.1.45}$$

$$F_{p_{\eta_2}} = \left(\frac{p_{\eta_1}^2}{m_{\eta_1}} - k_B T \right). \tag{4.1.46}$$

Operators with the form

$$\mathcal{L}_i = \left(-\frac{p_k}{m_k} p_i + F_{p_i} \right) \frac{\partial}{\partial p_i}, \tag{4.1.47}$$

as seen in $\mathcal{L}_B$ can be expanded following the derivation in Appendix A were we find

$$e^{\tau \mathcal{L}_i} p_i = p_i e^{-\tau (p_k/m_k)} + \tau F_{p_i} e^{-\tau (p_k/2m_k)} \left(\tau \frac{p_k}{2m_k} \right)^{-1} sinh \left[\tau \frac{p_k}{2m_k} \right]. \tag{4.1.48}$$

The function $\left(\tau\frac{p_k}{2m_k}\right)^{-1} sinh\left[\tau\frac{p_k}{2m_k}\right]$ is treated through an eighth order expansion.

A propagator

$$U_\alpha(\tau) = exp\left[\tau\mathcal{L}_\alpha\right], \tag{4.1.49}$$

for $\alpha = 1, \ldots, 5$ is associated with each Liouville piece. The Nosé-Hoover chain propagator can be written explicitly using the symmetric Trotter formula as follows

$$\begin{aligned} U(\tau) &= U_5\left(\frac{\tau}{2}\right) U_4\left(\frac{\tau}{2}\right) U_3\left(\frac{\tau}{2}\right) U_2\left(\frac{\tau}{2}\right), \\ &\times U_1(\tau)\, U_2\left(\frac{\tau}{2}\right) U_3\left(\frac{\tau}{2}\right) U_4\left(\frac{\tau}{2}\right) U_5\left(\frac{\tau}{2}\right). \end{aligned} \tag{4.1.50}$$

Using the direct translation technique, the pseudo-code form of the time-reversible algorithm is:

$$p_{\eta_2} \rightarrow p_{\eta_2} + \tfrac{\tau}{2} F_{p_{\eta_2}} \Big\} : U_5\left(\tfrac{\tau}{2}\right)$$

$$\left.\begin{aligned} p_{\eta_1} \;\rightarrow\; & p_{\eta_1} e^{-\frac{\tau}{4}\left(p_{\eta_2}/m_{\eta_2}\right)} + \tfrac{\tau}{4} F_{\eta_1} e^{-\frac{\tau}{4}\left(p_{\eta_2}/2m_{\eta_2}\right)} \left(\tfrac{\tau}{4}\tfrac{p_{\eta_2}}{2m_{\eta_2}}\right)^{-1} sinh\left[\tfrac{\tau}{4}\tfrac{p_{\eta_2}}{2m_{\eta_2}}\right] \end{aligned}\right\} : U_4\left(\tfrac{\tau}{2}\right)$$

$$\left.\begin{aligned} p_i \;\rightarrow\; & p_i \cdot exp\left[-\tfrac{\tau}{2}\tfrac{p_{\eta_1}}{m_{\eta_1}}\right] \end{aligned}\right\} : U_3\left(\tfrac{\tau}{2}\right)$$

$$\left.\begin{aligned} p_i \;\rightarrow\; & p_i \; + \tfrac{\tau}{2} F_i(q) \end{aligned}\right\} : U_2\left(\tfrac{\tau}{2}\right)$$

$$\left.\begin{aligned} q_i &\rightarrow q_i + \tau\tfrac{p_i}{m_i} \\ \eta_1 &\rightarrow \eta_1 + \tau\tfrac{p_{\eta_1}}{m_{\eta_1}} \\ \eta_2 &\rightarrow \eta_2 + \tau\tfrac{p_{\eta_2}}{m_{\eta_2}} \end{aligned}\right\} : U_1(\tau)$$

$$p_i \rightarrow p_i + \frac{\tau}{2} F_i(q) \Big\} : U_2\left(\frac{\tau}{2}\right)$$

$$p_i \rightarrow p_i \cdot exp\left[-\frac{\tau}{2}\frac{p_{\eta_1}}{m_{\eta_1}}\right] \Big\} : U_3\left(\frac{\tau}{2}\right)$$

$$p_{\eta_1} \rightarrow p_{\eta_1} e^{-\frac{\tau}{4}\left(p_{\eta_2}/m_{\eta_2}\right)} + \frac{\tau}{4} F_{\eta_1} e^{-\frac{\tau}{4}\left(p_{\eta_2}/2m_{\eta_2}\right)} \left(\frac{\tau}{4}\frac{p_{\eta_2}}{2m_{\eta_2}}\right)^{-1} sinh\left[\frac{\tau}{4}\frac{p_{\eta_2}}{2m_{\eta_2}}\right] \Big\} : U_4\left(\frac{\tau}{2}\right)$$

$$p_{\eta_2} \rightarrow p_{\eta_2} + \frac{\tau}{2} F_{p_{\eta_2}} \Big\} : U_5\left(\frac{\tau}{2}\right)$$

4.1.3 Time-reversible integration of Bulgac-Kusnezov dynamics

The Hamiltonian for the Bulgac-Kusnezov dynamics is given as

$$\mathcal{H}^{BK} = \sum_{i=1}^{N} \frac{p_i^2}{2m_i} + V(q) + \frac{p_\zeta^2}{2m_\zeta} + \frac{p_\xi^2}{2m_\xi} + Nk_BT\zeta + Nk_BT\xi, \qquad (4.1.51)$$

where (q, p) are the coordinates and momenta respectively. m is the oscillator mass, while ζ and ξ are the Bulgac-Kusnezov 'demons' with the corresponding fictitious masses m_ζ and m_ξ, and their associated momenta p_ζ and p_ξ. k_B is the Boltzmann constant whereas T is the temperature.

The equations of motion are given by

$$\dot{q}_i = \frac{p_i}{m_i} - q_i \frac{p_\xi}{m_\xi}, \tag{4.1.52}$$

$$\dot{\zeta} = \frac{p_\zeta}{m_\zeta}, \tag{4.1.53}$$

$$\dot{\xi} = \frac{p_\xi}{m_\xi}, \tag{4.1.54}$$

$$\dot{p}_i = F_i - p_i \frac{p_\zeta}{m_\zeta}, \tag{4.1.55}$$

$$\dot{p}_\zeta = \sum_{i=1}^{N} \left(\frac{p_i^2}{m_i} - k_B T \right), \tag{4.1.56}$$

$$\dot{p}_\xi = -\sum_{i=1}^{N} \left(q_i F_i + k_B T \right). \tag{4.1.57}$$

The Liouville operator $\mathcal{L}$ is associated with the equations of motion Eqs. (4.1.52) - (4.1.57), and split as

$$\mathcal{L} = \sum_{\alpha=1}^{5} \mathcal{L}_\alpha, \tag{4.1.58}$$

where the single terms are given as follows

$$\mathcal{L}_1 = \sum_{i=1}^{N} \left(-q_i \frac{p_\xi}{m_\xi} + \frac{p_i}{m} \right) \frac{\partial}{\partial q_i} + \frac{p_\xi}{m_\xi} \frac{\partial}{\partial \xi} + \frac{p_\zeta}{m_\zeta} \frac{\partial}{\partial \zeta}, \tag{4.1.59}$$

$$\mathcal{L}_2 = \sum_{i=1}^{N} F_i \frac{\partial}{\partial p_i}, \tag{4.1.60}$$

$$\mathcal{L}_3 = -\sum_{i=1}^{N} p_i \frac{p_\zeta}{m_\zeta} \frac{\partial}{\partial p_i}, \tag{4.1.61}$$

$$\mathcal{L}_4 = F_\xi \frac{\partial}{\partial p_\xi}, \tag{4.1.62}$$

$$\mathcal{L}_5 = F_\zeta \frac{\partial}{\partial p_\zeta}, \tag{4.1.63}$$

where we have defined the following

$$F_i = -\frac{\partial V}{\partial q_i}, \tag{4.1.64}$$

$$F_\xi = \sum_{i=1}^{N} \left(-q_i F_i - k_B T\right), \tag{4.1.65}$$

$$F_\zeta = \sum_{i=1}^{N} \left(\frac{p_i^2}{m_i} - k_B T\right). \tag{4.1.66}$$

A propagator

$$U_\alpha(\tau) = exp\left[\tau \mathcal{L}_\alpha\right], \tag{4.1.67}$$

for $\alpha = 1, \ldots, 5$ is associated with each Liouville piece. The Bulgac-Kusnezov propagator can be written explicitly using the symmetric Trotter formula as follows

$$\begin{aligned} U(\tau) &= U_5\left(\frac{\tau}{2}\right) U_4\left(\frac{\tau}{2}\right) U_3\left(\frac{\tau}{2}\right) U_2\left(\frac{\tau}{2}\right), \\ &\times U_1(\tau)\, U_2\left(\frac{\tau}{2}\right) U_3\left(\frac{\tau}{2}\right) U_4\left(\frac{\tau}{2}\right) U_5\left(\frac{\tau}{2}\right). \end{aligned} \tag{4.1.68}$$

Using the direct translation technique, the pseudo-code form of the time-reversible algorithm is:

$$p_\zeta \rightarrow p_\zeta + \tfrac{\tau}{2} F_\zeta \Big\} : U_5\left(\tfrac{\tau}{2}\right)$$

$$p_\xi \rightarrow p_\xi + \tfrac{\tau}{2} F_\xi \Big\} : U_4\left(\tfrac{\tau}{2}\right)$$

$$p_i \rightarrow p_i \cdot exp\left[-\tfrac{\tau}{2} \tfrac{p_\zeta}{m_\zeta}\right] \Big\} : U_3\left(\tfrac{\tau}{2}\right)$$

$$p_i \rightarrow p_i + \tfrac{\tau}{2} F_i \Big\} : U_2\left(\tfrac{\tau}{2}\right)$$

$$\left.\begin{array}{rcl} \zeta & \rightarrow & \zeta + \tau \frac{p_\zeta}{m_\zeta} \\ \xi & \rightarrow & \xi + \tau \frac{p_\xi}{m_\xi} \\ q_i & \rightarrow & q_i e^{-\tau(p_\xi/m_\xi)} + \tau \left(\frac{p_i}{m_i}\right) e^{-\tau(p_\xi/2m_\xi)} \left(\tau \frac{p_\xi}{2m_\xi}\right)^{-1} sinh\left[\tau \frac{p_\xi}{2m_\xi}\right] \end{array}\right\} : U_1(\tau)$$

$$p_i \rightarrow p_i + \tfrac{\tau}{2} F_i \Big\} : U_2\left(\tfrac{\tau}{2}\right)$$

$$p_i \rightarrow p_i \cdot exp\left[-\tfrac{\tau}{2} \frac{p_\zeta}{m_\zeta}\right] \Big\} : U_3\left(\tfrac{\tau}{2}\right)$$

$$p_\xi \rightarrow p_\xi + \tfrac{\tau}{2} F_\xi \Big\} : U_4\left(\tfrac{\tau}{2}\right)$$

$$p_\zeta \rightarrow p_\zeta + \tfrac{\tau}{2} F_\zeta \Big\} : U_5\left(\tfrac{\tau}{2}\right)$$

4.2 Measure-preserving algorithms

Ezra [20] proposed a method for deriving integrators which are both time-reversible and measure-preserving. In his proposal, instead of implementing an arbitrary splitting of the Liouville operator, one starts off with a splitting the Hamiltonian into a sum of n_s terms,

$$H = \sum_{\alpha=1}^{n_s} H(\alpha), \tag{4.2.1}$$

where the splitting (4.2.1) is not unique.

The equations of motion is readily established as

$$\dot{x} = \sum_{\alpha=1}^{n_s} \dot{x}(\alpha), \tag{4.2.2}$$

where

$$\dot{x}_i(\alpha) = \sum_j \mathcal{B}_{ij} \frac{\partial H(\alpha)}{\partial x_j}. \tag{4.2.3}$$

As a consequence of the split Hamiltonian, the split Liouville operator is given by

$$\mathcal{L} = \sum_{\alpha=1}^{n_s} \mathcal{L}_\alpha, \tag{4.2.4}$$

where

$$\mathcal{L} = \sum_{\alpha} \sum_{i,j} \mathcal{B}_{ij} \frac{\partial H(\alpha)}{\partial x_j} \frac{\partial}{\partial x_i}. \tag{4.2.5}$$

The phase space flow defined by Eq. (3.0.2) has non-zero compressibility, thus the statistical mechanics must be formulated in terms of a modified phase space measure[4, 5, 15, 35]

$$\bar{\omega} = e^{-\omega(x)}\omega, \tag{4.2.6}$$

where

$$\omega = dx^1 \wedge dx^2 \wedge \cdots \wedge dx^{2N}, \tag{4.2.7}$$

is the volume element in phase spaceG. S. Ezra [20] and the statistical weight $\omega(x)$ is defined by

$$\frac{d\omega}{dt} = \kappa(x). \tag{4.2.8}$$

It has been shown [20] that if,

$$\frac{\partial}{\partial x_j}\left[e^{-\omega(x)}\mathcal{B}_{ij}\right] = 0 \tag{4.2.9}$$

for $i = 1, \ldots, 2N$, then

$$\mathcal{L}_\alpha \bar{\omega} = 0, \tag{4.2.10}$$

for every α. This implies that propagators defined as

$$U_\alpha(\tau) = exp\left[\tau \mathcal{L}_\alpha\right], \tag{4.2.11}$$

where $\alpha = 1, 2, 3 \ldots n_s$, results in single propagation steps that preserve the phase space measure[41]. Moreover, using the symmetric Trotter factorization, algorithms that are both time-reversible and measure-preserving can derived from the complete propagator,

$$U(\tau) = U_1\left(\frac{\tau}{2}\right) \cdots U_{n_s-1}\left(\frac{\tau}{2}\right) \cdot U_{n_s}(\tau) \cdot U_{n_s-1}\left(\frac{\tau}{2}\right) \cdots U_1\left(\frac{\tau}{2}\right) + \mathcal{O}\left(\tau^3\right). \tag{4.2.12}$$

.

In the next sections we shall illustrate the derivation of measure-preserving integration algorithms for the Nosé-Hoover, Nosé-Hoover chain and Bulgac-Kusnezov dynamics.

4.2.1 Reversible measure-preserving integration of Nosé-Hoover dynamics

The Hamiltonian of Nosé-Hoover dynamics is given by

$$\mathcal{H}^{NH} = \sum_{i=1}^{N} \frac{p_i^2}{2m_i} + V(q) + \frac{p_\eta^2}{2m_\eta} + N k_B T \eta, \tag{4.2.13}$$

where (q, p) are the coordinates and momenta respectively. m is the oscillator mass, while η is the thermostat variable with the corresponding fictitious mass

m_η with its associated momenta p_η. k_B is the Boltzmann constant whereas T is the temperature.

The equations of motion of the dynamics can be defined as

$$\dot{q}_i = \frac{p_i}{m_i}, \tag{4.2.14}$$

$$\dot{p}_i = F_i - \frac{p_\eta}{m_\eta} p_i, \tag{4.2.15}$$

$$\dot{\eta} = \frac{p_\eta}{m_\eta}, \tag{4.2.16}$$

$$\dot{p}_\eta = \sum_{i=1}^{N} \left(\frac{p_i^2}{m_i} - k_B T \right), \tag{4.2.17}$$

Following Eq. (4.2.1), the Hamiltonian can be split into four terms as follows

$$H(1) = V(q), \tag{4.2.18}$$

$$H(2) = \sum_{i=1}^{N} \frac{p_i^2}{2m_i}, \tag{4.2.19}$$

$$H(3) = N k_B T \eta, \tag{4.2.20}$$

$$H(4) = \frac{p_\eta^2}{2m_\eta}. \tag{4.2.21}$$

We can find the consequent splitting of the Liouville operator from

$$\mathcal{L}_\alpha = \sum_{i,j} \mathcal{B}_{ij} \frac{\partial H_\alpha}{\partial x_j} \frac{\partial}{\partial x_i}. \tag{4.2.22}$$

As a consequence of the splitting of the Hamiltonian, the corresponding Liouville pieces are (see Appendix C.1)

$$\mathcal{L}_1 = -\sum_{i=1}^{N} \frac{\partial V(q)}{\partial q_i} \frac{\partial}{\partial p_i}, \tag{4.2.23}$$

$$\mathcal{L}_2 = \sum_{i=1}^{N} \left(\frac{p_i}{m_i} \frac{\partial}{\partial q_i} + \frac{p_i^2}{m_i} \frac{\partial}{\partial p_\eta} \right), \tag{4.2.24}$$

$$\mathcal{L}_3 = -N k_B T \frac{\partial}{\partial p_\eta}, \tag{4.2.25}$$

$$\mathcal{L}_4 = -\sum_{i=1}^{N} p_i \frac{p_\eta}{m_\eta} \frac{\partial}{\partial p_i} + \frac{p_\eta}{m_\eta} \frac{\partial}{\partial \eta}. \tag{4.2.26}$$

The complete Liouville operator is

$$\mathcal{L} = \sum_{i=1}^{N} \frac{p_i}{m} \frac{\partial}{\partial q_i} - \sum_{i=1}^{N} \left[\frac{\partial V(q)}{\partial q_i} + p_i \frac{p_\eta}{m_\eta} \right] \frac{\partial}{\partial p_i} + \frac{p_\eta}{m_\eta} \frac{\partial}{\partial \eta} + \sum_{i=1}^{N} \left[\frac{p_i^2}{m} - k_B T \right] \frac{\partial}{\partial p_\eta}. \tag{4.2.27}$$

Commuting Liouville operators can be combined for the purpose of defining an efficient algorithm as follows

$$\mathcal{L}_A = \mathcal{L}_1, \tag{4.2.28}$$

$$= -\sum_{i=1}^{N} \frac{\partial V(q)}{\partial q_i} \frac{\partial}{\partial p_i}, \tag{4.2.29}$$

$$= \sum_{i=1}^{N} F_i \frac{\partial}{\partial p_i}, \tag{4.2.30}$$

$$\begin{aligned}
\mathcal{L}_B &= \mathcal{L}_2 + \mathcal{L}_3, && (4.2.31)\\
&= \sum_{i=1}^{N} \frac{p_i}{m_i}\frac{\partial}{\partial q_i} + \sum_{i=1}^{N}\left(\frac{p_i^2}{m_i} - k_B T\right)\frac{\partial}{\partial p_\eta}, && (4.2.32)\\
&= \sum_{i=1}^{N} \frac{p_i}{m_i}\frac{\partial}{\partial q_i} + F_{p_\eta}\frac{\partial}{\partial p_\eta}, && (4.2.33)
\end{aligned}$$

$$\begin{aligned}
\mathcal{L}_C &= \mathcal{L}_4, && (4.2.34)\\
&= -\sum_{i=1}^{N} p_i \frac{p_\eta}{m_\eta}\frac{\partial}{\partial p_i} + \frac{p_\eta}{m_\eta}\frac{\partial}{\partial \eta}, && (4.2.35)
\end{aligned}$$

where we have defined the following

$$\begin{aligned}
F_i(q) &= -\frac{\partial V(q)}{\partial q_i}, && (4.2.36)\\
F_{p_\eta} &= \sum_{i=1}^{N}\left(\frac{p_i^2}{m_i} - k_B T\right). && (4.2.37)
\end{aligned}$$

Defining

$$U_\alpha(\tau) = exp\left[\tau \mathcal{L}_\alpha\right], \tag{4.2.38}$$

where $\alpha = A, B, C$ one possible reversible measure-preserving integration algorithm for the Nosé-Hoover thermostat under the symmetric Trotter factorization is then

$$
\begin{aligned}
U(\tau) &= U_B\left(\frac{\tau}{4}\right) \cdot U_C\left(\frac{\tau}{2}\right) \cdot U_B\left(\frac{\tau}{4}\right) \cdot U_A(\tau), \\
&\times \; U_B\left(\frac{\tau}{4}\right) \cdot U_C\left(\frac{\tau}{2}\right) \cdot U_B\left(\frac{\tau}{4}\right).
\end{aligned} \tag{4.2.39}
$$

Using the direct translation technique the following pseudo code form of the algorithm can be obtained:

$$
\left.
\begin{array}{rcl}
q_i & \rightarrow & q_i + \frac{\tau}{4}\frac{p_i}{m_i} \\
p_\eta & \rightarrow & p_\eta + \frac{\tau}{4}\sum_{i=1}^{N}\left(\frac{p_i^2}{m_i} - k_B T\right)
\end{array}
\right\} : U_B\left(\tfrac{\tau}{4}\right)
$$

$$
\left.
\begin{array}{rcl}
p_i & \rightarrow & p_i \cdot exp\left[-\frac{\tau}{2}\frac{p_\eta}{m_\eta}\right] \\
\eta & \rightarrow & \eta + \frac{\tau}{2}\frac{p_\eta}{m_\eta}
\end{array}
\right\} : U_C\left(\tfrac{\tau}{2}\right)
$$

$$
\left.
\begin{array}{rcl}
q_i & \rightarrow & q_i + \frac{\tau}{4}\frac{p_i}{m_i} \\
p_\eta & \rightarrow & p_\eta + \frac{\tau}{4}\sum_{i=1}^{N}\left(\frac{p_i^2}{m_i} - k_B T\right)
\end{array}
\right\} : U_B\left(\tfrac{\tau}{4}\right)
$$

$$
\left.
p_i \rightarrow p_i + \tau \cdot F_i(q)
\right\} : U_A(\tau)
$$

$$
\left.
\begin{array}{rcl}
q_i & \rightarrow & q_i + \frac{\tau}{4}\frac{p_i}{m_i} \\
p_\eta & \rightarrow & p_\eta + \frac{\tau}{4}\sum_{i=1}^{N}\left(\frac{p_i^2}{m_i} - k_B T\right)
\end{array}
\right\} : U_B\left(\tfrac{\tau}{4}\right)
$$

$$
\left.
\begin{array}{rcl}
p_i & \rightarrow & p_i \cdot exp\left[-\frac{\tau}{2}\frac{p_\eta}{m_\eta}\right] \\
\eta & \rightarrow & \eta + \frac{\tau}{2}\frac{p_\eta}{m_\eta}
\end{array}
\right\} : U_C\left(\tfrac{\tau}{2}\right)
$$

$$
\left.
\begin{array}{rcl}
q_i & \rightarrow & q_i + \frac{\tau}{4}\frac{p_i}{m_i} \\
p_\eta & \rightarrow & p_\eta + \frac{\tau}{4}\sum_{i=1}^{N}\left(\frac{p_i^2}{m_i} - k_B T\right)
\end{array}
\right\} : U_B\left(\tfrac{\tau}{4}\right)
$$

4.2.2 Reversible measure-preserving integration of Nosé-Hoover chain dynamics

The Hamiltonian of Nosé-Hoover chain dynamics is given by

$$\mathcal{H}^{NHC} = \sum_{i=1}^{N} \frac{p_i^2}{2m_i} + V(q) + \frac{p_{\eta_1}^2}{2m_{\eta_1}} + \frac{p_{\eta_2}^2}{2m_{\eta_2}} + Nk_BT\eta_1 + k_BT\eta_2, \quad (4.2.40)$$

where (q, p) are the coordinates and momenta respectively. m is the oscillator mass, while η_1 and η_2 are the two thermostat variables with the corresponding fictitious masses m_{η_1} and m_{η_2}, and their associated momenta p_{η_1} and p_{η_2}. k_B is the Boltzmann constant whereas T is the temperature.

The equations of motion are given by

$$\begin{aligned}
\dot{q}_i &= \frac{p_i}{m_i}, & (4.2.41)\\
\dot{\eta}_1 &= \frac{p_{\eta_1}}{m_{\eta_1}}, & (4.2.42)\\
\dot{\eta}_2 &= \frac{p_{\eta_2}}{m_{\eta_2}}, & (4.2.43)\\
\dot{p}_i &= -\frac{\partial V(q)}{\partial q_i} - p_i\frac{p_{\eta_1}}{m_{\eta_1}}, & (4.2.44)\\
\dot{p}_{\eta_1} &= \sum_{i=1}^{N}\left(\frac{p_i^2}{m_i} - k_BT\right) - p_{\eta_1}\frac{p_{\eta_2}}{m_{\eta_2}}, & (4.2.45)\\
\dot{p}_{\eta_2} &= \frac{p_{\eta_1}^2}{m_{\eta_1}} - k_BT. & (4.2.46)
\end{aligned}$$

Following Eq. (4.2.1), the Hamiltonian can be split into the following six terms

$$
\begin{aligned}
H(1) &= V(q), && (4.2.47)\\
H(2) &= \sum_{i=1}^{N} \frac{p_i^2}{2m_i}, && (4.2.48)\\
H(3) &= N k_B T \eta_1, && (4.2.49)\\
H(4) &= \frac{p_{\eta_1}^2}{2m_{\eta_1}}, && (4.2.50)\\
H(5) &= k_B T \eta_2, && (4.2.51)\\
H(6) &= \frac{p_{\eta_2}^2}{2m_{\eta_2}}. && (4.2.52)
\end{aligned}
$$

We can find the consequent splitting of the Liouville operator from

$$
\mathcal{L}_\alpha = \sum_{i,j} \mathcal{B}_{ij} \frac{\partial H_\alpha}{\partial x_j} \frac{\partial}{\partial x_i}. \tag{4.2.53}
$$

As a consequence of the splitting of the Hamiltonian, the corresponding Liouville pieces are (see Appendix C.2)

$$
\begin{aligned}
\mathcal{L}_1 &= -\sum_{i=1}^{N} \frac{\partial V(q)}{\partial q_i} \frac{\partial}{\partial p_i}, && (4.2.54)\\
\mathcal{L}_2 &= \sum_{i=1}^{N} \left(\frac{p_i}{m_i} \frac{\partial}{\partial q_i} + \frac{p_i^2}{m_i} \frac{\partial}{\partial p_{\eta_1}} \right), && (4.2.55)\\
\mathcal{L}_3 &= -N k_B T \frac{\partial}{\partial p_{\eta_1}}, && (4.2.56)\\
\mathcal{L}_4 &= -\sum_{i=1}^{N} p_i \frac{p_{\eta_1}}{m_{\eta_1}} \frac{\partial}{\partial p_i} + \frac{p_{\eta_1}}{m_{\eta_1}} \frac{\partial}{\partial \eta_1} + \frac{p_{\eta_1}^2}{m_{\eta_1}} \frac{\partial}{\partial p_{\eta_2}}, && (4.2.57)\\
\mathcal{L}_5 &= -k_B T \frac{\partial}{\partial p_{\eta_2}}, && (4.2.58)\\
\mathcal{L}_6 &= -p_{\eta_1} \frac{p_{\eta_2}}{m_{\eta_2}} \frac{\partial}{\partial p_{\eta_1}} + \frac{p_{\eta_2}}{m_{\eta_2}} \frac{\partial}{\partial \eta_2}. && (4.2.59)
\end{aligned}
$$

An efficient algorithm can be defined as a result of combining commuting

Liouville operators as follows

$$\begin{aligned}\mathcal{L}_A &= \mathcal{L}_1, \\ &= -\sum_{i=1}^{N} \frac{\partial V(q)}{\partial q_i} \frac{\partial}{\partial p_i}, \\ &= \sum_{i=1}^{N} F_i(q) \frac{\partial}{\partial p_i}, \end{aligned} \tag{4.2.60}$$

$$\begin{aligned}\mathcal{L}_B &= \mathcal{L}_2 + \mathcal{L}_3 + \mathcal{L}_6, \\ &= \sum_{i=1}^{N} \frac{p_i}{m_i} \frac{\partial}{\partial q_i} + \left[-p_{\eta_1} \frac{p_{\eta_2}}{m_{\eta_2}} + \sum_{i=1}^{N} \left(\frac{p_i^2}{m_i} - k_B T \right) \right] \frac{\partial}{\partial p_{\eta_1}} + \frac{p_{\eta_2}}{m_{\eta_2}} \frac{\partial}{\partial \eta_2}, \\ &= \sum_{i=1}^{N} \frac{p_i}{m_i} \frac{\partial}{\partial q_i} + \left[-p_{\eta_1} \frac{p_{\eta_2}}{m_{\eta_2}} + F_{p_{\eta_1}} \right] \frac{\partial}{\partial p_{\eta_1}} + \frac{p_{\eta_2}}{m_{\eta_2}} \frac{\partial}{\partial \eta_2}, \end{aligned} \tag{4.2.61}$$

$$\begin{aligned}\mathcal{L}_C &= \mathcal{L}_4 + \mathcal{L}_5, \\ &= -\sum_{i=1}^{N} p_i \frac{p_{\eta_1}}{m_{\eta_1}} \frac{\partial}{\partial p_i} + \frac{p_{\eta_1}}{m_{\eta_1}} \frac{\partial}{\partial \eta_1} + \sum_{i=1}^{N} \left(\frac{p_{\eta_1}^2}{m_{\eta_1}} - k_B T \right) \frac{\partial}{\partial p_{\eta_2}}, \\ &= -\sum_{i=1}^{N} p_i \frac{p_{\eta_1}}{m_{\eta_1}} \frac{\partial}{\partial p_i} + \frac{p_{\eta_1}}{m_{\eta_1}} \frac{\partial}{\partial \eta_1} + F_{p_{\eta_2}} \frac{\partial}{\partial p_{\eta_2}}, \end{aligned} \tag{4.2.62}$$

where we have defined the following

$$F_i(q) = -\frac{\partial V(q)}{\partial q_i}, \tag{4.2.63}$$

$$F_{p_{\eta_1}} = \sum_{i=1}^{N}\left(\frac{p_i^2}{m_i} - k_B T\right), \tag{4.2.64}$$

$$F_{p_{\eta_2}} = \frac{p_{\eta_1}^2}{m_{\eta_1}} - k_B T. \tag{4.2.65}$$

Operators with the form

$$\mathcal{L}_i = \left(-\frac{p_k}{m_k}p_i + F_{p_i}\right)\frac{\partial}{\partial p_i}, \tag{4.2.66}$$

as seen in $\mathcal{L}_B$ can be expanded following the derivation seen in Appendix A were we find

$$e^{\tau\mathcal{L}_i}p_i = p_i e^{-\tau(p_k/m_k)} + \tau F_{p_i} e^{-\tau(p_k/2m_k)}\left(\tau\frac{p_k}{2m_k}\right)^{-1} sinh\left[\tau\frac{p_k}{2m_k}\right]. \tag{4.2.67}$$

The function $\left(\tau\frac{p_k}{2m_k}\right)^{-1} sinh\left[\tau\frac{p_k}{2m_k}\right]$ is estimated using an eighth order expansion.

Defining

$$U_\alpha(\tau) = exp\left[\tau\mathcal{L}_\alpha\right], \tag{4.2.68}$$

where $\alpha = A, B, C$ one possible reversible measure-preserving integration algorithm for the Nosé-Hoover chain thermostat under the symmetric Trotter factorization is then

$$
\begin{aligned}
U(\tau) &= U_B\left(\frac{\tau}{4}\right)\cdot U_C\left(\frac{\tau}{2}\right)\cdot U_B\left(\frac{\tau}{4}\right)\cdot U_A(\tau), \\
&\times\ U_B\left(\frac{\tau}{4}\right)\cdot U_C\left(\frac{\tau}{2}\right)\cdot U_B\left(\frac{\tau}{4}\right). \qquad (4.2.69)
\end{aligned}
$$

Using the direct translation technique the following a pseudo code form of the algorithm can be obtained:

$$
\left.\begin{array}{rcc}
q_i & \rightarrow & q_i + \frac{\tau}{4}\frac{p_i}{m_i} \\
\eta_2 & \rightarrow & \eta_2 + \frac{\tau}{4}\frac{p_{\eta_2}}{m_{\eta_2}} \\
p_{\eta_1} & \rightarrow & p_{\eta_1} e^{-\frac{\tau}{4}\left(p_{\eta_2}/m_{\eta_2}\right)} + \frac{\tau}{4} F_{\eta_1} e^{-\frac{\tau}{4}\left(p_{\eta_2}/2m_{\eta_2}\right)} \left(\frac{\tau}{4}\frac{p_{\eta_2}}{2m_{\eta_2}}\right)^{-1} sinh\left[\frac{\tau}{4}\frac{p_{\eta_2}}{2m_{\eta_2}}\right] \\
& & U_B\left(\frac{\tau}{4}\right)
\end{array}\right\} :
$$

$$
\left.\begin{array}{rcc}
p_i & \rightarrow & p_i \cdot exp\left[-\frac{\tau}{2}\frac{p_{\eta_1}}{m_{\eta_1}}\right] \\
\eta_1 & \rightarrow & \eta_1 + \frac{\tau}{2}\frac{p_{\eta_1}}{m_{\eta_1}} \\
p_{\eta_2} & \rightarrow & p_{\eta_2} + \frac{\tau}{2}\left(\frac{p_{\eta_1}^2}{m_{\eta_1}} - k_B T\right)
\end{array}\right\} : U_C\left(\frac{\tau}{2}\right)
$$

$$
\left.\begin{array}{rcc}
q_i & \rightarrow & q_i + \frac{\tau}{4}\frac{p_i}{m_i} \\
\eta_2 & \rightarrow & \eta_2 + \frac{\tau}{4}\frac{p_{\eta_2}}{m_{\eta_2}} \\
p_{\eta_1} & \rightarrow & p_{\eta_1} e^{-\frac{\tau}{4}\left(p_{\eta_2}/m_{\eta_2}\right)} + \frac{\tau}{4} F_{\eta_1} e^{-\frac{\tau}{4}\left(p_{\eta_2}/2m_{\eta_2}\right)} \left(\frac{\tau}{4}\frac{p_{\eta_2}}{2m_{\eta_2}}\right)^{-1} sinh\left[\frac{\tau}{4}\frac{p_{\eta_2}}{2m_{\eta_2}}\right] \\
& & U_B\left(\frac{\tau}{4}\right)
\end{array}\right\} :
$$

$$
\left.\begin{array}{rcc}
p_i & \rightarrow & p_i + \tau\ \cdot F_i(q)
\end{array}\right\} : U_A(\tau)
$$

$$
\left.\begin{array}{rcc}
q_i & \rightarrow & q_i + \frac{\tau}{4}\frac{p_i}{m_i} \\
\eta_2 & \rightarrow & \eta_2 + \frac{\tau}{4}\frac{p_{\eta_2}}{m_{\eta_2}} \\
p_{\eta_1} & \rightarrow & p_{\eta_1} e^{-\frac{\tau}{4}\left(p_{\eta_2}/m_{\eta_2}\right)} + \frac{\tau}{4} F_{\eta_1} e^{-\frac{\tau}{4}\left(p_{\eta_2}/2m_{\eta_2}\right)} \left(\frac{\tau}{4}\frac{p_{\eta_2}}{2m_{\eta_2}}\right)^{-1} sinh\left[\frac{\tau}{4}\frac{p_{\eta_2}}{2m_{\eta_2}}\right] \\
& & U_B\left(\frac{\tau}{4}\right)
\end{array}\right\} :
$$

$$\left.\begin{array}{rcl} p_i & \rightarrow & p_i \cdot exp\left[-\frac{\tau}{2}\frac{p_{\eta_1}}{m_{\eta_1}}\right] \\ \eta_1 & \rightarrow & \eta_1 + \frac{\tau}{2}\frac{p_{\eta_1}}{m_{\eta_1}} \\ p_{\eta_2} & \rightarrow & p_{\eta_2} + \frac{\tau}{2}\left(\frac{p_{\eta_1}^2}{m_{\eta_1}} - k_B T\right) \end{array}\right\} : U_C\left(\frac{\tau}{2}\right)$$

$$\left.\begin{array}{rcl} q_i & \rightarrow & q_i + \frac{\tau}{4}\frac{p_i}{m_i} \\ \eta_2 & \rightarrow & \eta_2 + \frac{\tau}{4}\frac{p_{\eta_2}}{m_{\eta_2}} \\ p_{\eta_1} & \rightarrow & p_{\eta_1} e^{-\frac{\tau}{4}\left(p_{\eta_2}/m_{\eta_2}\right)} + \frac{\tau}{4} F_{\eta_1} e^{-\frac{\tau}{4}\left(p_{\eta_2}/2m_{\eta_2}\right)} \left(\frac{\tau}{4}\frac{p_{\eta_2}}{2m_{\eta_2}}\right)^{-1} sinh\left[\frac{\tau}{4}\frac{p_{\eta_2}}{2m_{\eta_2}}\right] \end{array}\right\} :$$
$$U_B\left(\frac{\tau}{4}\right)$$

4.2.3 Reversible measure-preserving integration of Bulgac-Kusnezov dynamics

The Hamiltonian of the Bulgac-Kusnezov dynamics is given by

$$\mathcal{H}^{BK} = \sum_{i=1}^{N} \frac{p_i^2}{2m_i} + V(q) + \frac{p_\zeta^2}{2m_\zeta} + \frac{p_\xi^2}{2m_\xi} + Nk_B T\zeta + Nk_B T\xi, \qquad (4.2.70)$$

where (q, p) are the coordinates and momenta respectively. m_i is the $i-th$ mass, while ζ and ξ are the Bulgac-Kusnezov 'demons' with the corresponding fictitious masses m_ζ and m_ξ, and their associated momenta p_ζ and p_ξ. k_B is the Boltzmann constant whereas T is the temperature.

The equations of motion are given by

$$\dot{q}_i = \frac{p_i}{m_i} - q_i \frac{p_\xi}{m_\xi}, \tag{4.2.71}$$

$$\dot{\zeta} = \frac{p_\zeta}{m_\zeta}, \tag{4.2.72}$$

$$\dot{\xi} = \frac{p_\xi}{m_\xi}, \tag{4.2.73}$$

$$\dot{p}_i = F_i - p_i \frac{p_\zeta}{m_\zeta}, \tag{4.2.74}$$

$$\dot{p}_\zeta = \sum_{i=1}^{N} \left(\frac{p_i^2}{m_i} - k_B T \right), \tag{4.2.75}$$

$$\dot{p}_\xi = -\sum_{i=1}^{N} \left(q_i F_i + k_B T \right). \tag{4.2.76}$$

Following Eq. (4.2.1), the Hamiltonian can be split into six terms as follows,

$$H(1) = V(q), \tag{4.2.77}$$

$$H(2) = \sum_{i=1}^{N} \frac{p_i^2}{2m_i}, \tag{4.2.78}$$

$$H(3) = N k_B T \zeta, \tag{4.2.79}$$

$$H(4) = N k_B T \xi, \tag{4.2.80}$$

$$H(5) = \frac{p_\zeta^2}{2m_\zeta}, \tag{4.2.81}$$

$$H(6) = \frac{p_\xi^2}{2m_\xi}. \tag{4.2.82}$$

We can find the consequent splitting of the Liouville operator from

$$\mathcal{L}_\alpha = \sum_{i,j} \mathcal{B}_{ij} \frac{\partial H_\alpha}{\partial x_j} \frac{\partial}{\partial x_i}. \tag{4.2.83}$$

As a consequence of splitting the Hamiltonian the split Liouville operator is (see Appendix C.3)

$$\mathcal{L}_1 = \sum_{i=1}^{N}\left(-\frac{\partial V(q)}{\partial q_i}\frac{\partial}{\partial p_i}+q_i\frac{\partial V(q)}{\partial q_i}\frac{\partial}{\partial p_\xi}\right), \tag{4.2.84}$$

$$\mathcal{L}_2 = \sum_{i=1}^{N}\left(\frac{p_i}{m_i}\frac{\partial}{\partial q_i}+\frac{p_i^2}{m_i}\frac{\partial}{\partial p_\zeta}\right), \tag{4.2.85}$$

$$\mathcal{L}_3 = -Nk_BT\frac{\partial}{\partial p_\zeta}, \tag{4.2.86}$$

$$\mathcal{L}_4 = -Nk_BT\frac{\partial}{\partial p_\xi}, \tag{4.2.87}$$

$$\mathcal{L}_5 = \frac{p_\zeta}{m_\zeta}\frac{\partial}{\partial \zeta}-\sum_{i=1}^{N}\frac{p_\zeta}{m_\zeta}p_i\frac{\partial}{\partial p_i}, \tag{4.2.88}$$

$$\mathcal{L}_6 = \frac{p_\xi}{m_\xi}\frac{\partial}{\partial \xi}-\sum_{i=1}^{N}\frac{p_\xi}{m_\xi}q_i\frac{\partial}{\partial q_i}. \tag{4.2.89}$$

For the purpose of defining an efficient integration algorithm, we can combine commuting Liouville operators as follows:

$$\begin{aligned}\mathcal{L}_A &= \mathcal{L}_1+\mathcal{L}_4,\\ &= -\sum_{i=1}^{N}\frac{\partial V(q)}{\partial q_i}\frac{\partial}{\partial p_i}+\sum_{i=1}^{N}\left[q_i\frac{\partial V(q)}{\partial q_i}-k_BT\right]\frac{\partial}{\partial p_\xi},\\ &= \sum_{i=1}^{N}F_i(q)\frac{\partial}{\partial p_i}+F_{p_\xi}\frac{\partial}{\partial p_\xi},\end{aligned} \tag{4.2.90}$$

$$\begin{aligned}\mathcal{L}_B &= \mathcal{L}_2+\mathcal{L}_3,\\ &= \sum_{i=1}^{N}\frac{p_i}{m_i}\frac{\partial}{\partial q_i}+\sum_{i=1}^{N}\left[\frac{p_i^2}{m_i}-k_BT\right]\frac{\partial}{\partial p_\zeta},\\ &= \sum_{i=1}^{N}\frac{p_i}{m_i}\frac{\partial}{\partial q_i}+F_{p_\zeta}\frac{\partial}{\partial p_\zeta},\end{aligned} \tag{4.2.91}$$

$$\begin{aligned}\mathcal{L}_C &= \mathcal{L}_5 + \mathcal{L}_6, \\ &= \frac{p_\zeta}{m_\zeta}\frac{\partial}{\partial \zeta} - \sum_{i=1}^{N}\frac{p_\zeta}{m_\zeta}p_i\frac{\partial}{\partial p_i} + \frac{p_\xi}{m_\xi}\frac{\partial}{\partial \xi} - \sum_{i=1}^{N}\frac{p_\xi}{m_\xi}q_i\frac{\partial}{\partial q_i}, \end{aligned} \tag{4.2.92}$$

where we have defined the following

$$F_i(q) = -\frac{\partial V(q)}{\partial q_i}, \tag{4.2.93}$$

$$F_{P_\xi} = \sum_{i=1}^{N}\left(q_i\frac{\partial V(q)}{\partial q_i} - k_B T\right), \tag{4.2.94}$$

$$F_{p_\zeta} = \sum_{i=1}^{N}\left(\frac{p_i^2}{m} - k_B T\right). \tag{4.2.95}$$

Defining

$$U_\alpha(\tau) = exp\left[\tau\mathcal{L}_\alpha\right], \tag{4.2.96}$$

where $\alpha = A, B, C$ one possible reversible measure-preserving integration algorithm for the Bulgac-Kusnezov thermostat under the symmetric Trotter factorization is then

$$\begin{aligned}U(\tau) &= U_B\left(\frac{\tau}{4}\right)\cdot U_C\left(\frac{\tau}{2}\right)\cdot U_B\left(\frac{\tau}{4}\right)\cdot U_A(\tau), \\ &\times\ U_B\left(\frac{\tau}{4}\right)\cdot U_C\left(\frac{\tau}{2}\right)\cdot U_B\left(\frac{\tau}{4}\right).\end{aligned} \tag{4.2.97}$$

Using the direct translation technique the following a pseudo code form of the algorithm can be obtained:

$$\left.\begin{array}{rcl} q_i & \rightarrow & q_i + \frac{\tau}{4}\frac{p_i}{m_i} \\ p_\zeta & \rightarrow & p_\zeta + \frac{\tau}{4}F_{p_\zeta} \end{array}\right\} : U_B\left(\frac{\tau}{4}\right)$$

$$\left.\begin{array}{rcl} p_i & \rightarrow & p_i \cdot exp\left[-\frac{\tau}{2}\frac{p_\zeta}{m_\zeta}\right] \\ q_i & \rightarrow & q_i \cdot exp\left[-\frac{\tau}{2}\frac{p_\xi}{m_\xi}\right] \\ \zeta & \rightarrow & \zeta + \frac{\tau}{2}\frac{p_\zeta}{m_\zeta} \\ \xi & \rightarrow & \xi + \frac{\tau}{2}\frac{p_\xi}{m_\xi} \end{array}\right\} : U_C\left(\frac{\tau}{2}\right)$$

$$\left.\begin{array}{rcl} q_i & \rightarrow & q_i + \frac{\tau}{4}\frac{p_i}{m_i} \\ p_\zeta & \rightarrow & p_\zeta + \frac{\tau}{4}F_{p_\zeta} \end{array}\right\} : U_B\left(\frac{\tau}{4}\right)$$

$$\left.\begin{array}{rcl} p_i & \rightarrow & p_i + \tau F_i \\ p_\xi & \rightarrow & p_\xi + \tau F_{p_\xi} \end{array}\right\} : U_A\left(\tau\right)$$

$$\left.\begin{array}{rcl} q_i & \rightarrow & q_i + \frac{\tau}{4}\frac{p_i}{m_i} \\ p_\zeta & \rightarrow & p_\zeta + \frac{\tau}{4}F_{p_\zeta} \end{array}\right\} : U_B\left(\frac{\tau}{4}\right)$$

$$\left.\begin{array}{rcl} p_i & \rightarrow & p_i \cdot exp\left[-\frac{\tau}{2}\frac{p_\zeta}{m_\zeta}\right] \\ q_i & \rightarrow & q_i \cdot exp\left[-\frac{\tau}{2}\frac{p_\xi}{m_\xi}\right] \\ \zeta & \rightarrow & \zeta + \frac{\tau}{2}\frac{p_\zeta}{m_\zeta} \\ \xi & \rightarrow & \xi + \frac{\tau}{2}\frac{p_\xi}{m_\xi} \end{array}\right\} : U_C\left(\frac{\tau}{2}\right)$$

$$\left.\begin{array}{rcl} q_i & \rightarrow & q_i + \frac{\tau}{4}\frac{p_i}{m_i} \\ p_\zeta & \rightarrow & p_\zeta + \frac{\tau}{4}F_{p_\zeta} \end{array}\right\} : U_B\left(\frac{\tau}{4}\right)$$

Chapter 5

Model

In this chapter, I shall study the stability and ergodic properties of the dynamics of the Nosé-Hoover chain and Bulgac-Kusnezov thermostats coupled to a one-dimensional harmonic oscillator using measure-preserving algorithms.

It is widely known that the Nosé-Hoover dynamics[7, 8, 33] does not sample uniformly all the regions of phase space. As a result the system fails to generate the correct canonical ensemble. However, this problem has been solved by introducing additional thermostat variables presented in the case of Nosé-Hoover chain dynamics[34, 42] . In the case of Bulgac-Kusnezov dynamics, Sergi and Ezra[43] have confirmed that the dynamics has some difficulties for producing the correct canonical distribution function.

In this chapter, we study the stability and ergodic properties of the dynamics of two deterministic thermostats; Nosé-Hoover chain and Bulgac-Kusnezov thermostats. This is done by coupling the thermostats to a harmonic oscillator in one dimension which is the typical model used to address the problem of ergodicity in the integration of the dynamics. Using previously formulated reversible measure-preserving algorithms (refer to previous chapter for derivations), we investigate the ability of our Nosé-Hoover chain and Bulgac-Kusnezov ther-

k	q	p	ξ	ζ	p_ξ	p_ζ
0.5	0.3	0.0	0.0	0.0	0.0	-3.0
1.0	0.3	0.0	0.0	0.0	0.0	0.0
1.5	0.3	0.0	0.0	0.0	1.0	-2.0
2.0	0.3	0.0	0.0	1.0	-2.0	-3.0
2.5	0.3	0.0	0.0	1.0	-3.0	-3.0
3.0	0.3	0.0	-0.5	0.0	0.0	2.7
3.5	0.3	0.0	2.0	0.0	0.0	2.7

Table 5.1: The table shows the initials values used with various k values for q, p, ξ, ζ, p_ξ and p_ζ at $t = 0$.

mostats to produce the correct canonical distribution functions. The choice to only investigate simulations using reversible measure-preserving algorithms is trivial, this is because algorithms formulated under time-reversible are not measure-preserving while algorithms formulated under measure-preserving are automatically time-reversible. Thus, the type of numerical calculations considered within this chapter will follow the general scheme for defining measure-preserving integrators in the case of the Nosé-Hoover chain and Bulgac-Kusnezov dynamics. The Hamiltonian used within this thesis is of the form

$$\mathcal{H} = \frac{p^2}{2m} + \frac{1}{2}\, k \cdot q^2, \tag{5.0.1}$$

where k is the spring constant.

Results and Discussions

During the simulation several values of k ranging from 0.5 to 3.5 were studied. The results reported within this chapter are for typical values of $k = 0.5$, $k = 1.0$, $k = 1.5$, $k = 2.0$, $k = 2.5$, $k = 3.0$ and $k = 3.5$ with the initial values indicated in table 5.1 at time $t = 0$.

The time step used during the simulations of the Nosé-Hoover chain and

Bulgac-Kusnezov dynamics was $\tau = 0.0025$, and all runs were calculated for 10^7 time steps using the reversible measure-preserving propagator defined by Eq. (4.2.12). Also, the values for all the masses and k_BT were taken to be 1.0.

It has been found that both the Nosé-Hoover chain and Bulgac-Kusnezov dynamics yield numerically stable integration schemes using the reversible measure-preserving algorithms. This can be seen by studying the long-term behavior of the normalized Hamiltonian function H for the two dynamics and noting that it fluctuates about 1.0. The normalized Hamiltonian function H for the Bulgac-Kusnezov dynamics fluctuates to the order of 10^{-2} as seen in Fig. 5.1 and 10^{-3} as seen in Fig. 5.4. In Fig. 5.7, Fig. 5.10, Fig. 5.13, Fig. 5.16 and Fig. 5.19, the Bulgac-Kusnezov Hamiltonian function has fluctuations which are of the order 10^{-4}. On the contrary, the Hamiltonian function for the Nosé-Hoover chain dynamics maintains a high level of accuracy throughout the plots with fluctuations of the order 10^{-6}.

In order to check if a particular dynamics samples the canonical distribution correctly, conservation of the energy function alone is not enough. Following the work of Sergi and Ferrario[5] and Sergi [15], a detailed way of calculating the radial dependence and visualizing it for sampling the phase space has been presented. In this thesis, the radial phase space probability of the Bulgac-Kusnezov dynamics (seen in Fig. 5.2, Fig. 5.5, Fig. 5.8, Fig. 5.11, Fig. 5.14, Fig. 5.17 and Fig. 5.20) and the Nosé-Hoover chain dynamics (seen in Fig. 5.3, Fig. 5.6, Fig. 5.9, Fig. 5.12, Fig. 5.15, Fig. 5.18 and Fig. 5.21) were calculated and compared to that of the harmonic oscillator since its canonical distribution is isotropic in phase space and it achieves an exact radial dependence.

Figure 5.2, Fig. 5.5, Fig. 5.8, Fig. 5.11, Fig. 5.14, Fig. 5.17 and Fig. 5.20 all show the comparison between the radial phase space probability for the Bulgac-Kusnezov dynamics and the harmonic oscillator. The Bulgac-Kusnezov dynamics is seen to have difficulties in producing the correct canonical distribu-

tion function as seen from its radial phase space probability plot. The graphs lack the general bell-like form seen from the radial phase space probability of the harmonic oscillator. Furthermore, the inset displays of the phase space distribution for the Bulgac-Kusnezov show that not all regions of the phase space are sampled uniformly throughout the system. Hence the dynamics is not ergodic.

Figure 5.3, Fig. 5.6, Fig. 5.9, Fig. 5.12, Fig. 5.15, Fig. 5.18 and Fig. 5.21 all show the comparison between the radial phase space probability for the Nosé-Hoover chain dynamics and the harmonic oscillator. The Nosé-Hoover chain dynamics is seen to produce the correct canonical distribution function as seen from its radial phase space probability plot. All the graphs have the general bell-like shape seen from the radial phase space probability of the harmonic oscillator. Furthermore, by analyzing the inset displays of the phase space distribution for the Nosé-Hoover chain, one can confirm that the dynamics samples uniformly all the regions of the phase space throughout the system. The dynamics is ergodic.

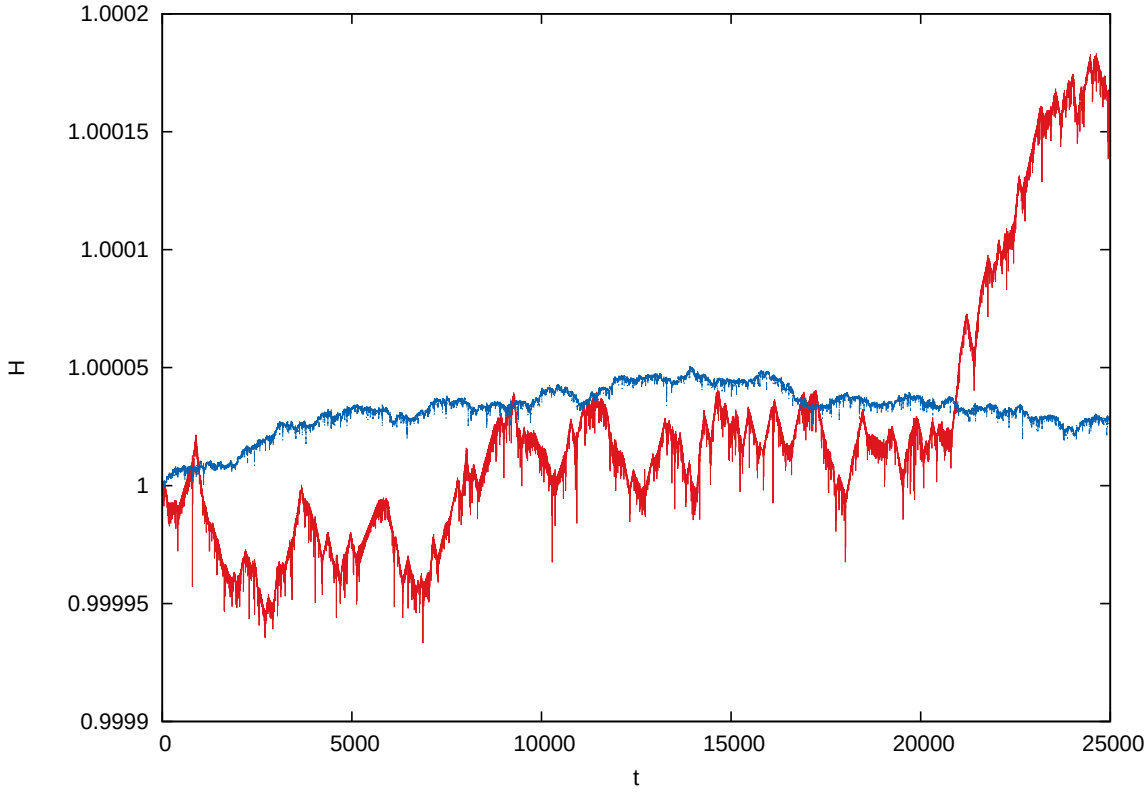

Fig. 5.1: Normalized energy function H versus time for the Bulgac-Kusnezov and Nosé-Hoover chain dynamics with initial conditions $q = 0.3$, $p = 0.0$, $\xi = 0.0$, $\zeta = 0.0$,$p_\xi = 0.0$, $p_\zeta = -3.0$ and $k = 0.5$ at $t = 0$. The energy function for the Bulgac-Kusnezov dynamics is displayed in red whereas the energy function for the Nosé-Hoover chain dynamics is represented in blue.

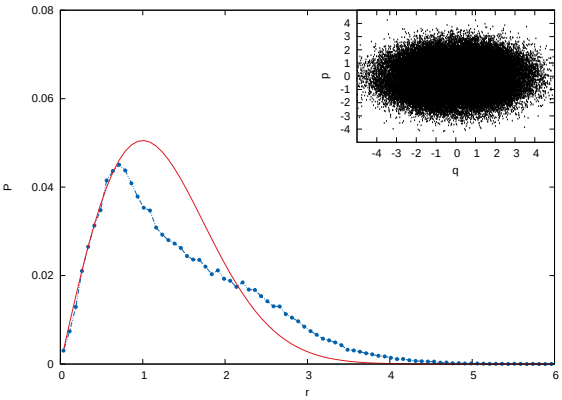

Fig. 5.2: Radial phase space probability for the Bulgac-Kusnezov dynamics with initial conditions $q = 0.3$, $p = 0.0$, $\xi = 0.0$, $\zeta = 0.0$,$p_\xi = 0.0$, $p_\zeta = -3.0$ and $k = 0.5$ at $t = 0$. Numerical results for the Bulgac-Kusnezov dynamics are shown using the blue bullets whereas the red line shows the theoretical value. The phase space distribution for this dynamics is displayed by the inset.

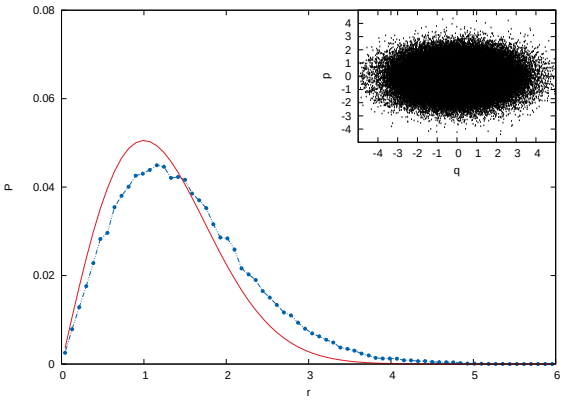

Fig. 5.3: Radial phase space probability for the Nosé-Hoover chain dynamics with initial conditions $q = 0.3$, $p = 0.0$, $\xi = 0.0$, $\zeta = 0.0$,$p_\xi = 0.0$, $p_\zeta = -3.0$ and $k = 0.5$ at $t = 0$. Numerical results for the Nosé-Hoover chain dynamics are shown using the blue bullets whereas the red line shows the theoretical value. The phase space distribution for this dynamics is displayed by the inset.

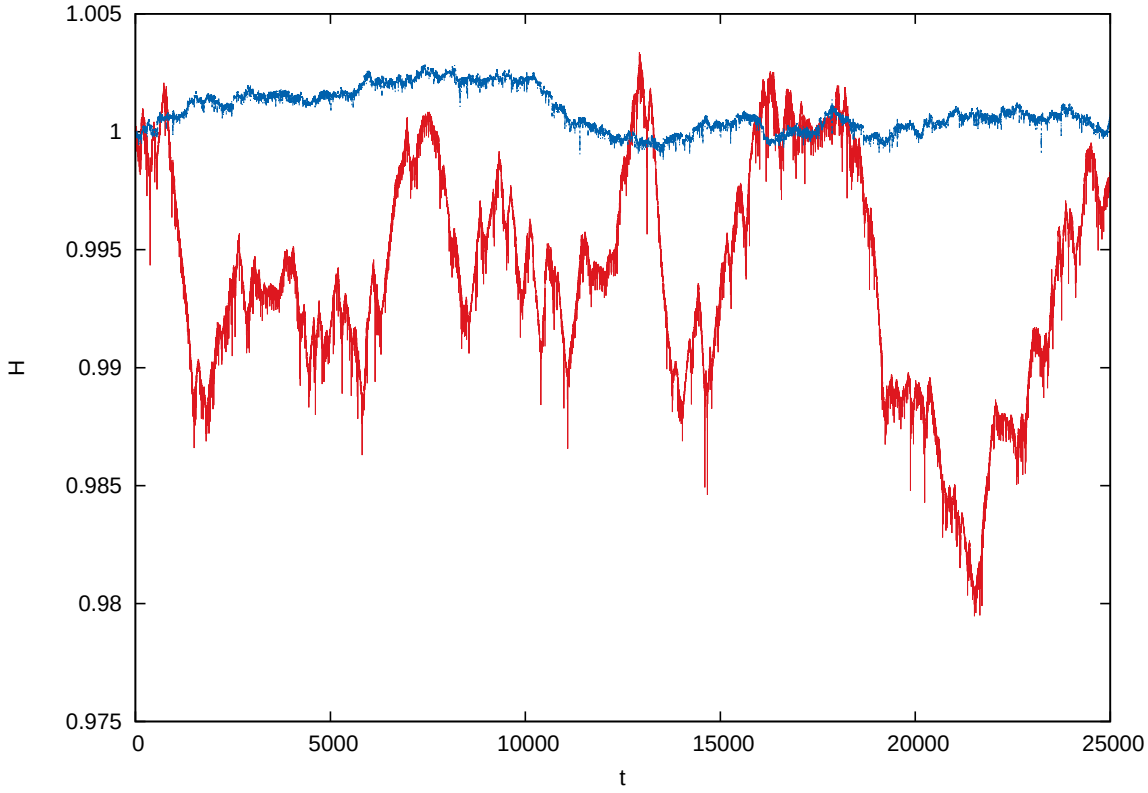

Fig. 5.4: Normalized energy function H versus time for the Bulgac-Kusnezov and Nosé-Hoover chain dynamics with initial conditions$q = 0.3$, $p = 0.0$, $\xi = 0.0$, $\zeta = 0.0$,$p_\xi = 0.0$, $p_\zeta = 0.0$ and $k = 1.0$ at $t = 0$. The energy function for the Bulgac-Kusnezov dynamics is displayed in red whereas the energy function for the Nosé-Hoover chain dynamics is represented in blue.

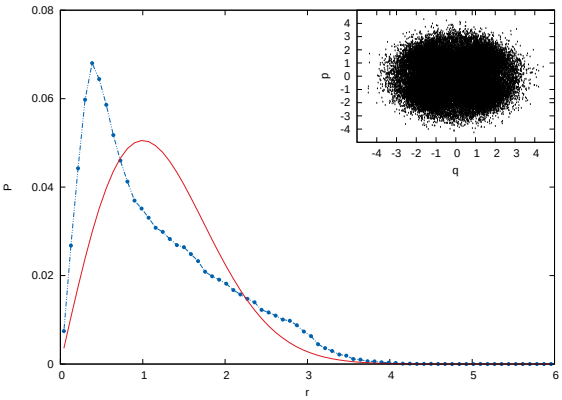

Fig. 5.5: Radial phase space probability for the Bulgac-Kusnezov dynamics with initial conditions $q = 0.3$, $p = 0.0$, $\xi = 0.0$, $\zeta = 0.0$,$p_\xi = 0.0$, $p_\zeta = 0.0$ and $k = 1.0$ at $t = 0$. Numerical results for the Bulgac-Kusnezov dynamics are shown using the blue bullets whereas the red line shows the theoretical value. The phase space distribution for this dynamics is displayed by the inset.

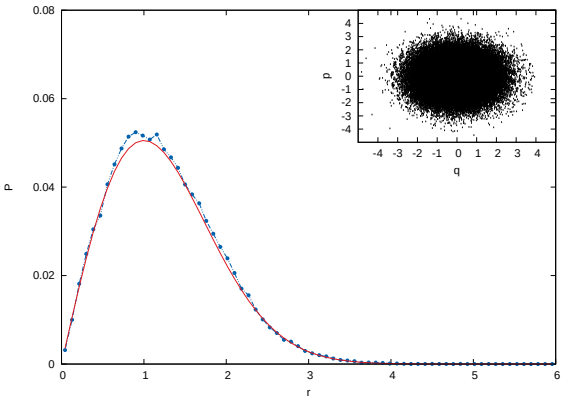

Fig. 5.6: Radial phase space probability for the Nosé-Hoover chain dynamics with initial conditions $q = 0.3$, $p = 0.0$, $\xi = 0.0$, $\zeta = 0.0$,$p_\xi = 0.0$, $p_\zeta = 0.0$ and $k = 1.0$ at $t = 0$. Numerical results for the Nosé-Hoover chain dynamics are shown using the blue bullets whereas the red line shows the theoretical value. The phase space distribution for this dynamics is displayed by the inset.

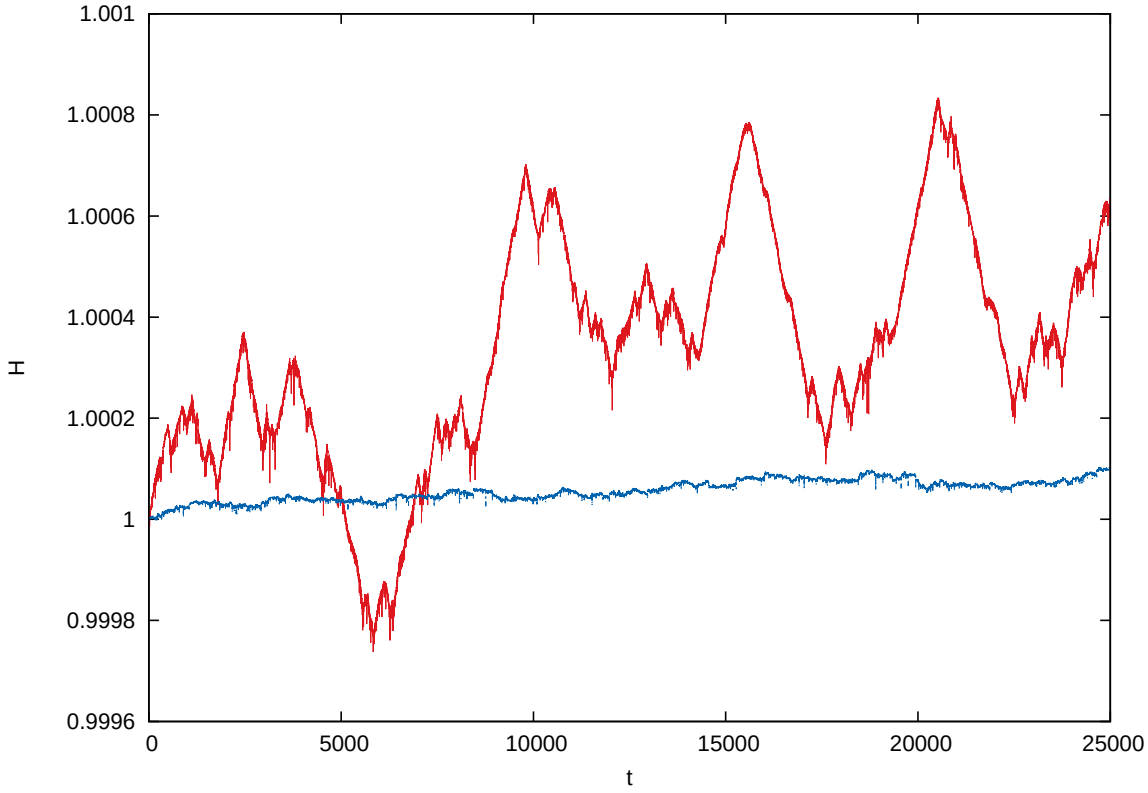

Fig. 5.7: Normalized energy function H versus time for the Bulgac-Kusnezov and Nosé-Hoover chain dynamics with initial conditions$q = 0.3$, $p = 0.0$, $\xi = 0.0$, $\zeta = 0.0$,$p_\xi = 1.0$, $p_\zeta = -2.0$ and $k = 1.5$ at $t = 0$. The energy function for the Bulgac-Kusnezov dynamics is displayed in red whereas the energy function for the Nosé-Hoover chain dynamics is represented in blue.

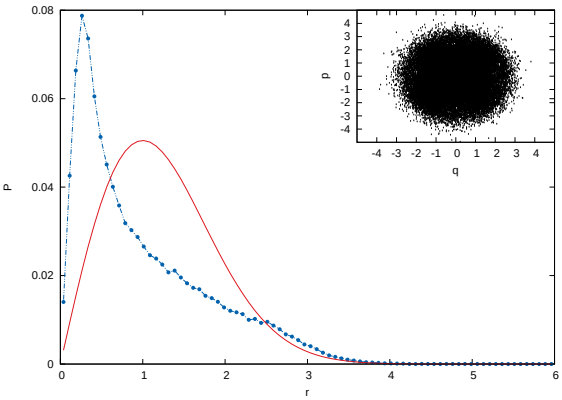

Fig. 5.8: Radial phase space probability for the Bulgac-Kusnezov dynamics with initial conditions $q = 0.3$, $p = 0.0$, $\xi = 0.0$, $\zeta = 0.0$,$p_\xi = 1.0$, $p_\zeta = -2.0$ and $k = 1.5$ at $t = 0$. Numerical results for the Bulgac-Kusnezov dynamics are shown using the blue bullets whereas the red line shows the theoretical value. The phase space distribution for this dynamics is displayed by the inset.

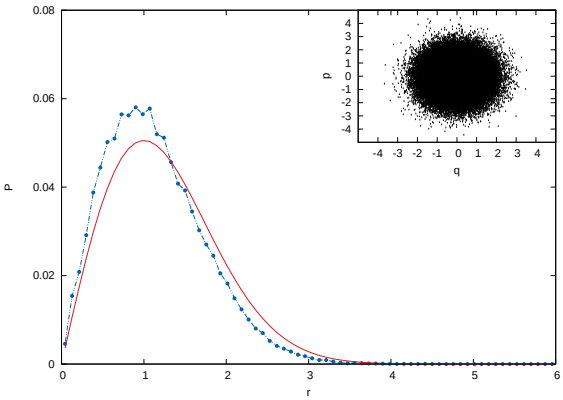

Fig. 5.9: Radial phase space probability for the Nosé-Hoover chain dynamics with initial conditions $q = 0.3$, $p = 0.0$, $\xi = 0.0$, $\zeta = 0.0$,$p_\xi = 1.0$, $p_\zeta = -2.0$ and $k = 1.5$ at $t = 0$. Numerical results for the Nosé-Hoover chain dynamics are shown using the blue bullets whereas the red line shows the theoretical value. The phase space distribution for this dynamics is displayed by the inset.

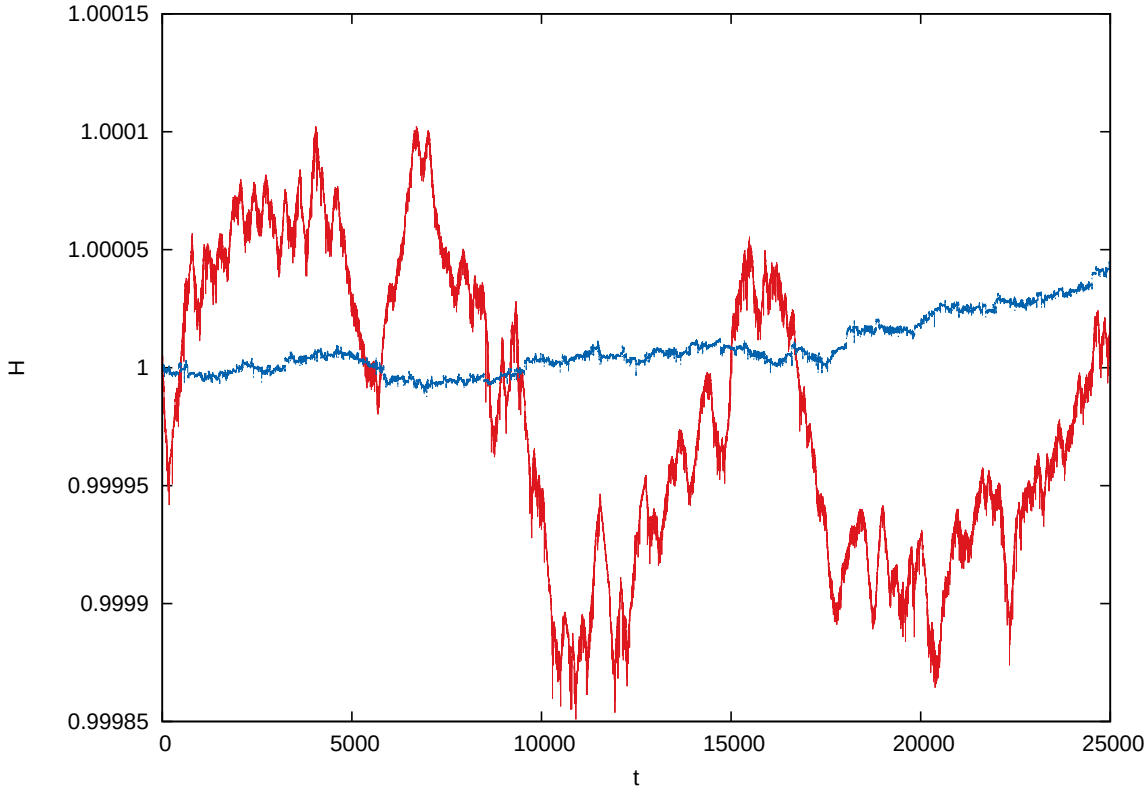

Fig. 5.10: Normalized energy function H versus time for the Bulgac-Kusnezov and Nosé-Hoover chain dynamics with initial conditions$q = 0.3$, $p = 0.0$, $\xi = 0.0$, $\zeta = 1.0$,$p_\xi = -2.0$, $p_\zeta = -3.0$ and $k = 2.0$ at $t = 0$. The energy function for the Bulgac-Kusnezov dynamics is displayed in red whereas the energy function for the Nosé-Hoover chain dynamics is represented in blue.

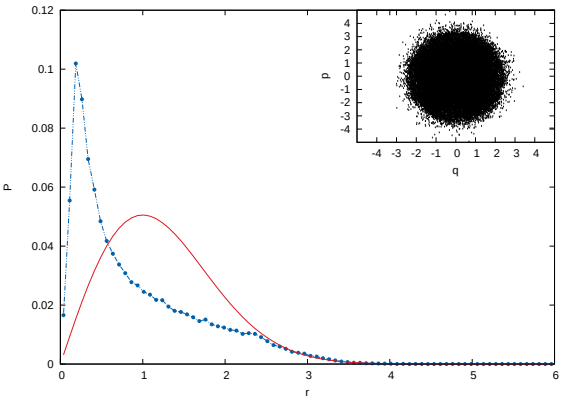

Fig. 5.11: Radial phase space probability for the Bulgac-Kusnezov dynamics with initial conditions $q = 0.3$, $p = 0.0$, $\xi = 0.0$, $\zeta = 1.0$, $p_\xi = -2.0$, $p_\zeta = -3.0$ and $k = 2.0$ at $t = 0$. Numerical results for the Bulgac-Kusnezov dynamics are shown using the blue bullets whereas the red line shows the theoretical value. The phase space distribution for this dynamics is displayed by the inset.

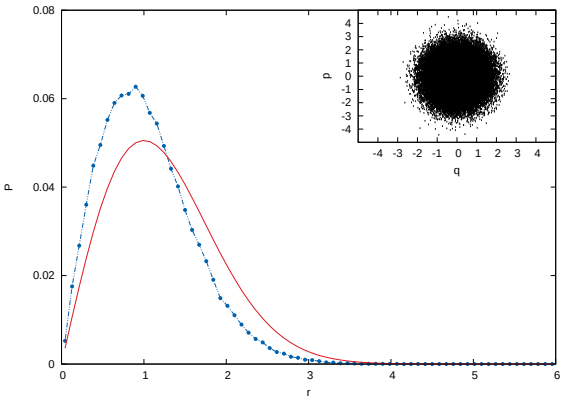

Fig. 5.12: Radial phase space probability for the Nosé-Hoover chain dynamics with initial conditions $q = 0.3$, $p = 0.0$, $\xi = 0.0$, $\zeta = 1.0$, $p_\xi = -2.0$, $p_\zeta = -3.0$ and $k = 2.0$ at $t = 0$. Numerical results for the Nosé-Hoover chain dynamics are shown using the blue bullets whereas the red line shows the theoretical value. The phase space distribution for this dynamics is displayed by the inset.

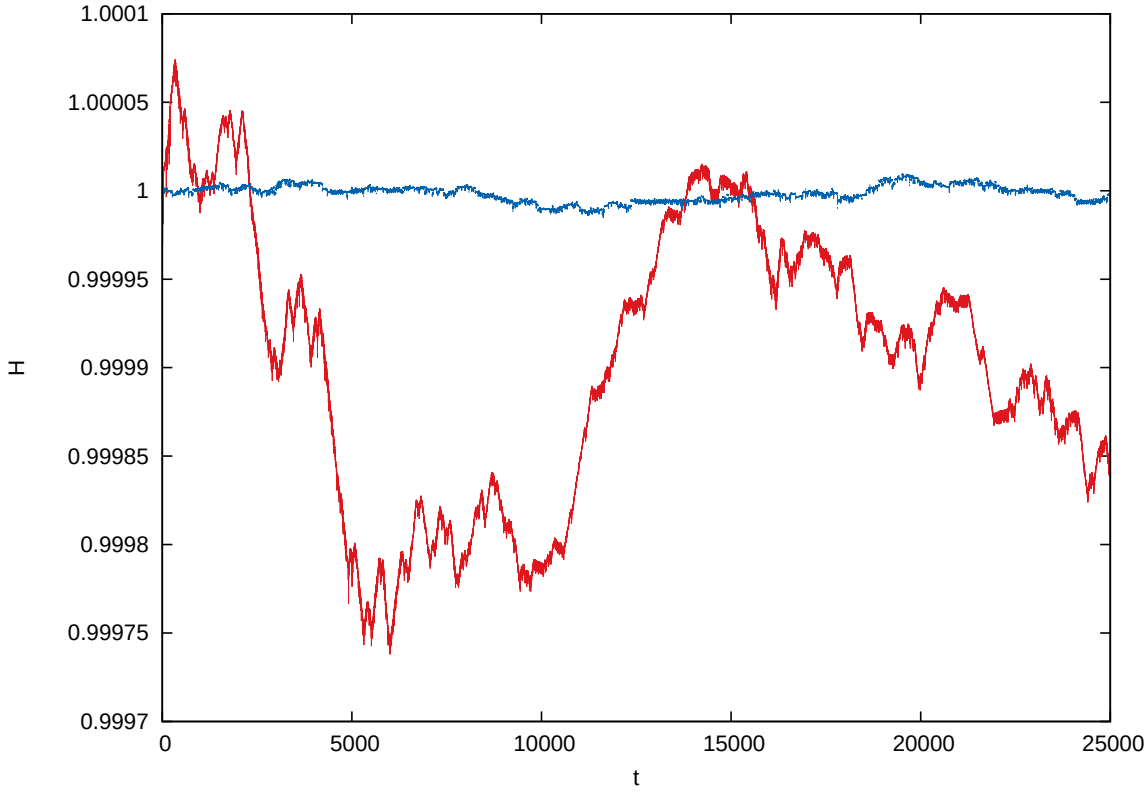

Fig. 5.13: Normalized energy function H versus time for the Bulgac-Kusnezov and Nosé-Hoover chain dynamics with initial conditions$q = 0.3$, $p = 0.0$, $\xi = 0.0$, $\zeta = 1.0$,$p_\xi = -3.0$, $p_\zeta = -3.0$ and $k = 2.5$ at $t = 0$. The energy function for the Bulgac-Kusnezov dynamics is displayed in red whereas the energy function for the Nosé-Hoover chain dynamics is represented in blue.

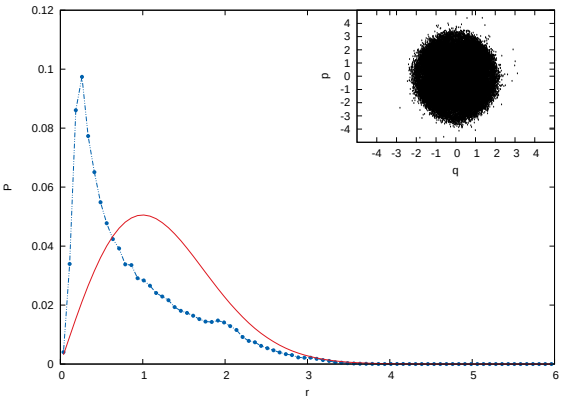

Fig. 5.14: Radial phase space probability for the Bulgac-Kusnezov dynamics with initial conditions $q = 0.3$, $p = 0.0$, $\xi = 0.0$, $\zeta = 1.0$, $p_\xi = -3.0$, $p_\zeta = -3.0$ and $k = 2.5$ at $t = 0$. Numerical results for the Bulgac-Kusnezov dynamics are shown using the blue bullets whereas the red line shows the theoretical value. The phase space distribution for this dynamics is displayed by the inset.

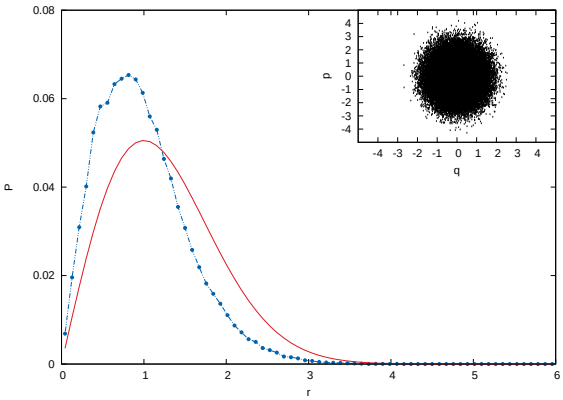

Fig. 5.15: Radial phase space probability for the Nosé-Hoover chain dynamics with initial conditions $q = 0.3$, $p = 0.0$, $\xi = 0.0$, $\zeta = 1.0$, $p_\xi = -3.0$, $p_\zeta = -3.0$ and $k = 2.5$ at $t = 0$. Numerical results for the Nosé-Hoover chain dynamics are shown using the blue bullets whereas the red line shows the theoretical value. The phase space distribution for this dynamics is displayed by the inset.

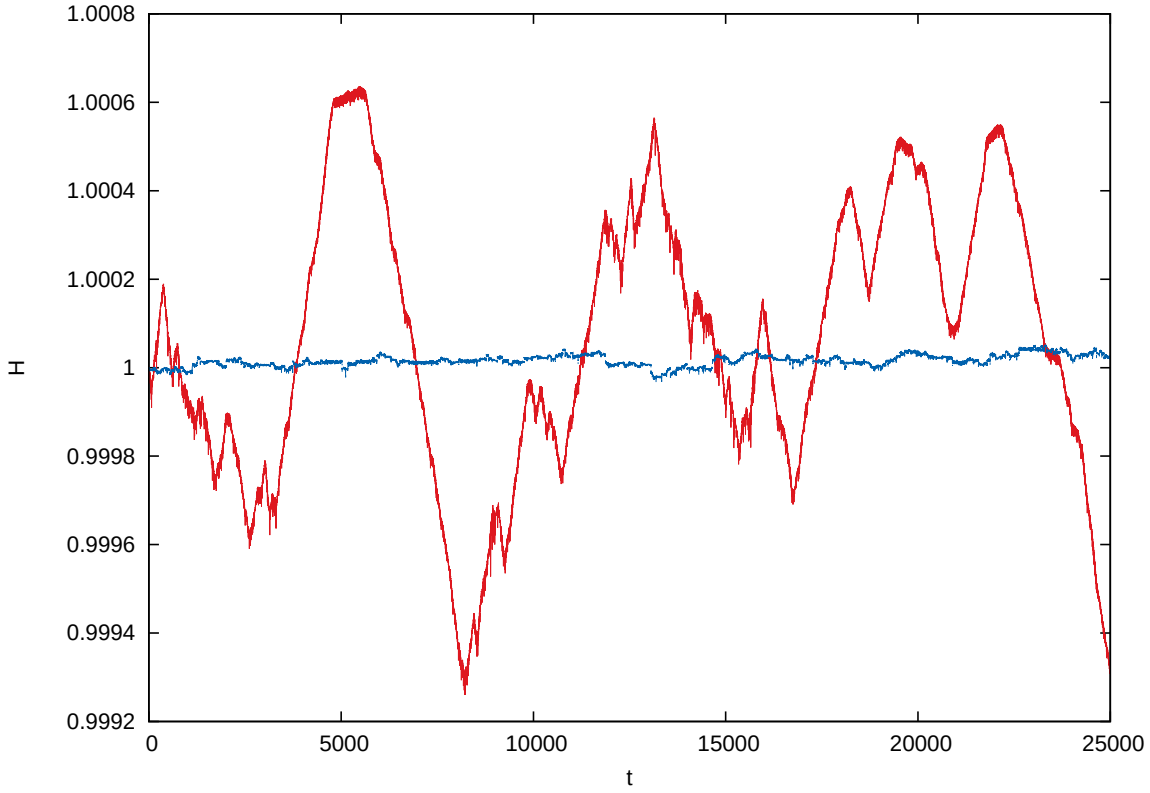

Fig. 5.16: Normalized energy function H versus time for the Bulgac-Kusnezov and Nosé-Hoover chain dynamics with initial conditions$q = 0.3$, $p = 0.0$, $\xi = -0.5$, $\zeta = 0.0$,$p_\xi = 0.0$, $p_\zeta = 2.7$ and $k = 3.0$ at $t = 0$. The energy function for the Bulgac-Kusnezov dynamics is displayed in red whereas the energy function for the Nosé-Hoover chain dynamics is represented in blue.

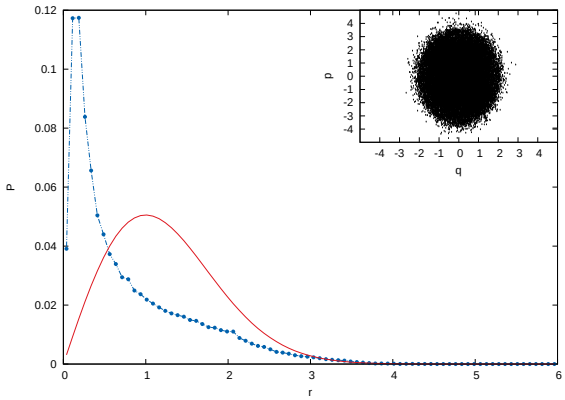

Fig. 5.17: Radial phase space probability for the Bulgac-Kusnezov dynamics with initial conditions $q = 0.3$, $p = 0.0$, $\xi = -0.5$, $\zeta = 0.0$,$p_\xi = 0.0$, $p_\zeta = 2.7$ and $k = 3.0$ at $t = 0$. Numerical results for the Bulgac-Kusnezov dynamics are shown using the blue bullets whereas the red line shows the theoretical value. The phase space distribution for this dynamics is displayed by the inset.

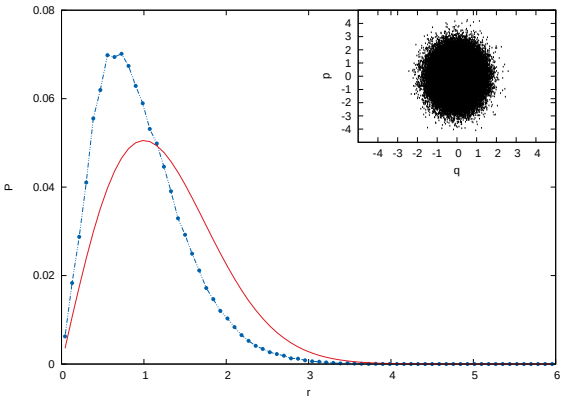

Fig. 5.18: Radial phase space probability for the Nosé-Hoover chain dynamics with initial conditions $q = 0.3$, $p = 0.0$, $\xi = -0.5$, $\zeta = 0.0$,$p_\xi = 0.0$, $p_\zeta = 2.7$ and $k = 3.0$ at $t = 0$. Numerical results for the Nosé-Hoover chain dynamics are shown using the blue bullets whereas the red line shows the theoretical value. The phase space distribution for this dynamics is displayed by the inset.

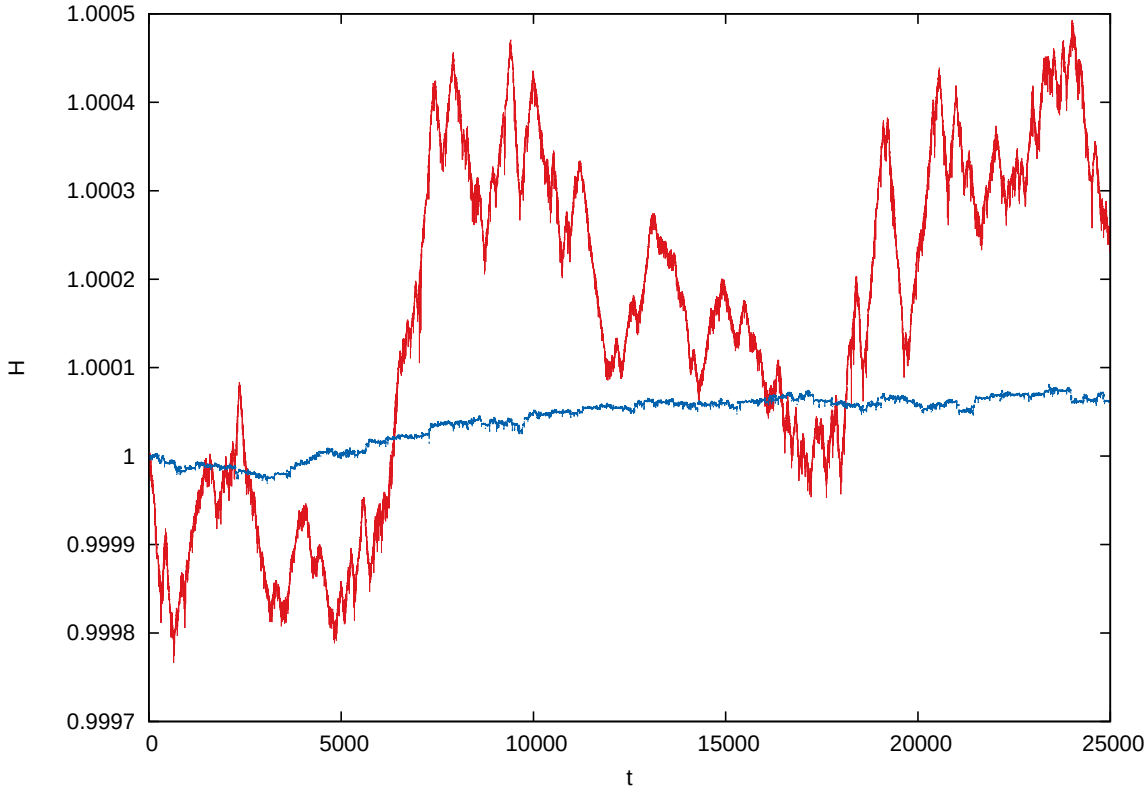

Fig. 5.19: Normalized energy function H versus time for the Bulgac-Kusnezov and Nosé-Hoover chain dynamics with initial conditions$q = 0.3$, $p = 0.0$, $\xi = 2.0$, $\zeta = 0.0$,$p_\xi = 0.0$, $p_\zeta = 2.7$ and $k = 3.5$ at $t = 0$. The energy function for the Bulgac-Kusnezov dynamics is displayed in red whereas the energy function for the Nosé-Hoover chain dynamics is represented in blue.

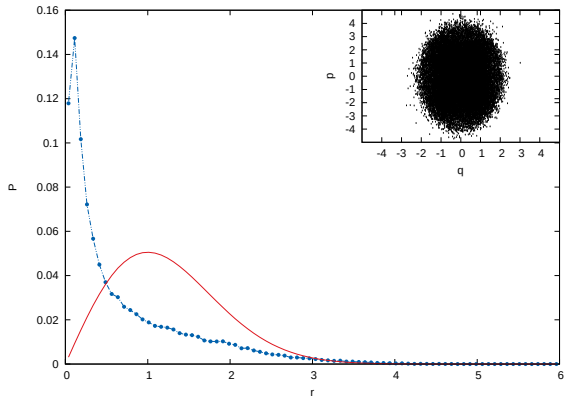

Fig. 5.20: Radial phase space probability for the Bulgac-Kusnezov dynamics with initial conditions $q = 0.3$, $p = 0.0$, $\xi = 2.0$, $\zeta = 0.0$,$p_\xi = 0.0$, $p_\zeta = 2.7$ and $k = 3.5$ at $t = 0$. Numerical results for the Bulgac-Kusnezov dynamics are shown using the blue bullets whereas the red line shows the theoretical value. The phase space distribution for this dynamics is displayed by the inset.

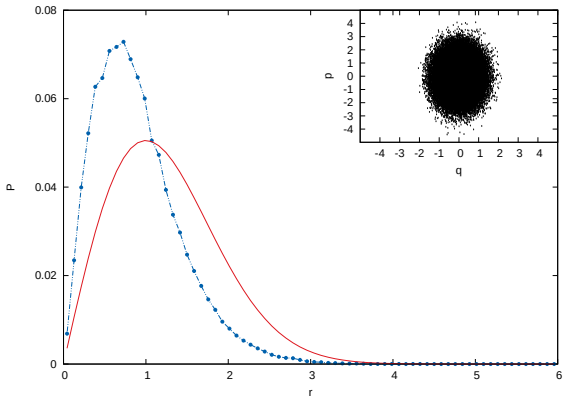

Fig. 5.21: Radial phase space probability for the Nosé-Hoover chain dynamics with initial conditions $q = 0.3$, $p = 0.0$, $\xi = 2.0$, $\zeta = 0.0$,$p_\xi = 0.0$, $p_\zeta = 2.7$ and $k = 3.5$ at $t = 0$. Numerical results for the Nosé-Hoover chain dynamics are shown using the blue bullets whereas the red line shows the theoretical value. The phase space distribution for this dynamics is displayed by the inset.

Chapter 6

Conclusions

Special techniques and algorithms are required to perform constant temperature MD simulations. This is because MD simulations are most naturally carried out in the microcanonical ensemble under constant energy conditions. In order to achieve a constant temperature constraints, the simulations have to be done in the canonical ensemble. Theoretically within Hamiltonian dynamics, this is achieved by coupling the system of interest with a thermal reservoir with an infinite number of degrees of freedom. With the finite computational resources available, infinite conditions cannot be represented on the computer. However, using non-Hamiltonian dynamics the thermal reservoir can be represented by just a few additional degrees of freedom. Such a methodology is known as the extended systems approach.

In this thesis, we have reviewed the algebraic formalism for non-Hamiltonian brackets [5, 15] in phase space for the following deterministic non-Hamiltonian thermostats; Nosé-Hoover, Nosé-Hoover chain and Bulgac-Kusnezov. Furthermore, we have derived the compressibility and shown how to build the invariant measure for these extended systems. Using non-Hamiltonian bracket structure presented by Sergi and Ferrario[5] and Sergi[15], we have shown how

to design efficient algorithms for integrating the equations of motion for the non-Hamiltonian thermostats considered in this thesis. The type of algorithms considered are time-reversible and measure-preserving in nature. We have presented a systematic approach to deriving time-reversible algorithms which were introduced by Tuckerman *et al*[16] using the Trotter symmetric factorization of the Liouville propagator. Moreover, by exploiting the non-Hamiltonian structure we have obtained measure-preserving integrators that automatically and exactly conserve the invariant measure. This latter approach was formulated by Ezra[20]. The resulting measure-preserving algorithms formulated from such integrators are found to be both measure-preserving and time-reversible. The algorithms have been derived for the following deterministic non-Hamiltonian thermostats; Nosé-Hoover, Nosé-Hoover chain and Bulgac-Kusnezov.

We have performed calculations for comparing the stability and ergodicity of the Nosé-Hoover chain and Bulgac-Kusnezov dynamics using a one dimensional harmonic oscillator integrated by means of measure-preserving algorithms. It has been found that both dynamics are stable. Moreover, when analyzing the case of the Nosé-Hoover chain, the dynamics is seen to be efficient in achieving the correct canonical distribution function by producing conserved energy functions when different initials conditions are used. However, in the case of the Bulgac-Kusnezov dynamics, it is necessary to adjust the initial conditions for achieving the correct canonical distribution function, even if the total Hamiltonian is correctly conserved in all cases.

The theory and techniques presented here for the derivation and implementation of algorithms for extended systems are of particular interest within MD simulations at constant temperature.

Future work will consist of extending the study to classical spin systems.

Appendix A

Operator formula

From the evolution equation (where $i \neq k$)

$$\int_0^\tau \left(-\frac{p_k}{m_k} p_i + F_{p_i} \right) \frac{\partial}{\partial p_i}, \tag{A.0.1}$$

one gets

$$\partial g\left(p_i\right) = \frac{\partial p_i}{-\frac{p_k}{m_k} p_i + F_{p_i}}, \tag{A.0.2}$$

and

$$\begin{aligned} g\left(p_i\right) &= \int \left(\frac{\partial p_i}{-\frac{p_k}{m_k} p_i + F_{p_i}} \right), \\ &= -\frac{m_k}{p_k} \int \left(\frac{\partial \left(-\frac{p_k}{m_k} p_i \right)}{-\frac{p_k}{m_k} p_i + F_{p_i}} \right), \\ &= -\frac{m_k}{p_k} \int \left(\frac{\partial \left(-\frac{p_k}{m_k} p_i + F_{p_i} \right)}{-\frac{p_k}{m_k} p_i + F_{p_i}} \right), \\ &= -\frac{m_k}{p_k} ln \left(-\frac{p_k}{m_k} p_i + F_{p_i} \right). \end{aligned} \tag{A.0.3}$$

Hence

$$\frac{\partial}{\partial g\left(p_i\right)} = \frac{\partial}{\partial\left[-\frac{m_k}{p_k} ln\left(-\frac{p_k}{m_k} p_i + F_{p_i}\right)\right]}, \tag{A.0.4}$$

and one finds

$$g\left(p_i\right) = -\frac{m_k}{p_k} ln\left(-\frac{p_k}{m_k} p_i + F_{p_i}\right). \tag{A.0.5}$$

In order to apply the following identity, an inverse of g has to be determined, hence for g,

$$\begin{aligned} p_i &= g^{-1}\left(g\left(p_i\right)\right), \\ &= -\frac{m_k}{p_k} exp\left(-\frac{p_k}{m_k} g\left(p_i\right)\right) + \frac{m_k}{p_k} F_{p_i}. \end{aligned} \tag{A.0.6}$$

Finally, we obtain

$$
\begin{aligned}
exp\left[\tau\left(-\frac{p_k}{m_k}p_i + F_{p_i}\right)\frac{\partial}{\partial p_i}\right]p_i &= exp\left[\tau\frac{\partial}{\partial\left[-\frac{m_k}{p_k}ln\left(-\frac{p_k}{m_k}p_i + F_{p_i}\right)\right]}\right]p_i, \\
&= -\frac{m_k}{p_k}exp\left[ln\left(-\frac{p_k}{m_k}p_i + F_{p_i}\right) - \tau\frac{p_k}{m_k}\right] + \frac{m_k}{p_k}F_{p_i}, \\
&= -\frac{m_k}{p_k}\left(-\frac{p_k}{m_k}p_i + F_{p_i}\right)e^{-\tau p_k/m_k} + \frac{m_k}{p_k}F_{p_i}, \\
&= p_i e^{-\tau p_k/m_k} + \frac{m_k}{p_k}F_{p_i}\left(1 - e^{-\tau p_k/m_k}\right), \\
&= p_i e^{-\tau p_k/m_k} + \frac{m_k}{p_k}F_{p_i}e^{-\tau p_k/2m_k}\left(e^{\tau p_k/2m_k} - e^{-\tau p_k/2m_k}\right), \\
&= p_i e^{-\tau p_k/m_k} + F_{p_i}e^{-\tau p_k/2m_k}\left(\frac{e^{\tau p_k/2m_k} - e^{-\tau p_k/2m_k}}{2\frac{p_k}{2m_k}}\right), \\
&= p_i e^{-\tau p_k/m_k} + \tau F_{p_i}e^{-\tau p_k/2m_k}\left(\frac{\sinh\left[\tau\frac{p_k}{2m_k}\right]}{\tau\frac{p_k}{2m_k}}\right).
\end{aligned}
\tag{A.0.7}
$$

Appendix B

Derivation of the invariant measure

B.1 Deriving the invariant measure for the Nosé-Hoover dynamics

The phase space compressibility of the Nosé-Hoover thermostat is

$$\begin{aligned} \kappa &= \sum_{i,j} \frac{\partial \mathcal{B}_{ij}^{NH}}{\partial x_i} \frac{\partial \mathcal{H}_{NH}}{\partial x_j}, \\ &= -\frac{p_\eta}{m_\eta}. \end{aligned} \tag{B.1.1}$$

Upon introducing the function

$$\mathcal{H}_T^{NH} = \mathcal{H} + \frac{p_\eta^2}{2m_\eta}, \tag{B.1.2}$$

one can easily find that

$$\kappa_{NH} = \frac{1}{k_B T} \frac{d\mathcal{H}_T^{NH}}{dt}, \tag{B.1.3}$$

so the invariant measure in phase space reads

$$\begin{aligned} d\mu &= dx\, exp\left[-\int_t dt \kappa_{NH}\right], \\ &= dx\, exp\left[-\beta \mathcal{H}_T^{NH}\right], \\ &= dx\, exp\left[-\beta \mathcal{H}_T^{NH}\right]\ exp\left[\eta\right], \end{aligned} \tag{B.1.4}$$

as desired.

B.2 Deriving the invariant measure for the Nosé-Hoover chain dynamics

The phase space compressibility of the Nosé-Hoover chain thermostat is

$$\begin{aligned} \kappa &= \sum_{i,j} \frac{\partial \mathcal{B}_{ij}^{NHC}}{\partial x_i} \frac{\partial \mathcal{H}_{NHC}}{\partial x_j}, \\ &= -\frac{p_\eta}{m_\eta} - \frac{p_\xi}{m_\xi}. \end{aligned} \tag{B.2.1}$$

Upon introducing the function

$$\mathcal{H}_T^{NHC} = \mathcal{H} + \frac{p_\eta^2}{2m_\eta} + \frac{p_\xi^2}{2m_\xi}, \tag{B.2.2}$$

one can easily find that

$$\kappa_{NHC} = \frac{1}{k_B T} \frac{d\mathcal{H}_T^{NHC}}{dt}, \tag{B.2.3}$$

so the invariant measure in phase space reads

$$\begin{aligned} d\mu &= dx\, exp\left[-\int_t dt \kappa_{NHC}\right], \\ &= dx\, exp\left[-\beta \mathcal{H}_T^{NHC}\right], \\ &= dx\, exp\left[-\beta \mathcal{H}_T^{NHC}\right]\ exp\left[\eta + \xi\right], \end{aligned} \tag{B.2.4}$$

as desired.

B.3 Deriving the invariant measure for the Bulgac-Kusnezov dynamics

The phase space compressibility of the Bulgac-Kusnezov thermostat is

$$\begin{aligned} \kappa &= \sum_{i,j} \frac{\partial \mathcal{B}_{ij}^{BK}}{\partial x_i} \frac{\partial \mathcal{H}_{BK}}{\partial x_j}, \\ &= -\frac{p_\zeta}{m_\zeta} - \frac{p_\xi}{m_\xi}. \end{aligned} \tag{B.3.1}$$

Upon introducing the function

$$\mathcal{H}_T^{BK} = \mathcal{H} + \frac{p_\zeta^2}{2m_\zeta} + \frac{p_\xi^2}{2m_\xi}, \tag{B.3.2}$$

one can easily find that

$$\kappa_{BK} = \frac{1}{k_B T} \frac{d\mathcal{H}_T^{BK}}{dt}, \tag{B.3.3}$$

so the invariant measure in phase space reads

$$\begin{aligned} d\mu &= dx\, exp\left[-\int_t dt \kappa_{BK}\right], \\ &= dx\, exp\left[-\beta \mathcal{H}_T^{BK}\right], \\ &= dx\, exp\left[-\beta \mathcal{H}_T^{BK}\right]\ exp\left[\zeta + \xi\right], \end{aligned} \tag{B.3.4}$$

as desired.

Appendix C

Derivation of the Liouville operator

C.1 Deriving the Liouville operator for the Nosé-Hoover dynamics

We can find the consequent splitting of the Liouville operator from

$$\mathcal{L}_\alpha = \sum_{i,j} \mathcal{B}_{ij} \frac{\partial H_\alpha}{\partial x_j} \frac{\partial}{\partial x_i}. \tag{C.1.1}$$

Thus

$$\begin{aligned} \mathcal{L}_1 &= \sum_{i,j} \mathcal{B}_{ij} \frac{\partial H_1}{\partial x_j} \frac{\partial}{\partial x_i} = \sum_{i,j} \mathcal{B}_{ij} \frac{\partial V(q)}{\partial x_j} \frac{\partial}{\partial x_i} = \sum_{i,j} \mathcal{B}_{i1} \frac{\partial V(q)}{\partial x_1} \frac{\partial}{\partial x_i}, \\ &= \mathcal{B}_{21} \frac{\partial V(q)}{\partial x_1} \frac{\partial}{\partial x_2}, \\ &= -\frac{\partial V(q)}{\partial q} \frac{\partial}{\partial p}, \end{aligned} \tag{C.1.2}$$

$$
\begin{aligned}
\mathcal{L}_2 &= \sum_{i,j} \mathcal{B}_{ij} \frac{\partial H_2}{\partial x_j} \frac{\partial}{\partial x_i} = \sum_{i,j} \mathcal{B}_{ij} \frac{\partial}{\partial x_j} \left(\frac{p^2}{2m} \right) \frac{\partial}{\partial x_i} = \sum_i \mathcal{B}_{i2} \frac{\partial}{\partial x_2} \left(\frac{p^2}{2m} \right) \frac{\partial}{\partial x_i}, \\
&= \mathcal{B}_{12} \frac{\partial}{\partial x_2} \left(\frac{p^2}{2m} \right) \frac{\partial}{\partial x_1} + \mathcal{B}_{42} \frac{\partial}{\partial x_2} \left(\frac{p^2}{2m} \right) \frac{\partial}{\partial x_4}, \\
&= \mathcal{B}_{12} \frac{\partial}{\partial p} \left(\frac{p^2}{2m} \right) \frac{\partial}{\partial q} + \mathcal{B}_{42} \frac{\partial}{\partial p} \left(\frac{p^2}{2m} \right) \frac{\partial}{\partial p_\eta}, \\
&= \frac{p}{m} \frac{\partial}{\partial q} + \frac{p^2}{m} \frac{\partial}{\partial p_\eta}, \qquad \text{(C.1.3)}
\end{aligned}
$$

$$
\begin{aligned}
\mathcal{L}_3 &= \sum_{i,j} \mathcal{B}_{ij} \frac{\partial H_3}{\partial x_j} \frac{\partial}{\partial x_i} = \sum_{i,j} \mathcal{B}_{ij} \frac{\partial \left(k_B T \eta \right)}{\partial x_j} \frac{\partial}{\partial x_i} = \sum_i \mathcal{B}_{i3} \frac{\partial \left(k_B T \eta \right)}{\partial x_3} \frac{\partial}{\partial x_i}, \\
&= \mathcal{B}_{43} \frac{\partial \left(k_B T \eta \right)}{\partial x_3} \frac{\partial}{\partial x_4} = \mathcal{B}_{43} \frac{\partial \left(k_B T \eta \right)}{\partial \eta} \frac{\partial}{\partial p_\eta}, \\
&= -k_B T \frac{\partial}{\partial p_\eta}, \qquad \text{(C.1.4)}
\end{aligned}
$$

$$
\begin{aligned}
\mathcal{L}_4 &= \sum_{i,j} \mathcal{B}_{ij} \frac{\partial H_4}{\partial x_j} \frac{\partial}{\partial x_i} = \sum_{i,j} \mathcal{B}_{ij} \frac{\partial}{\partial x_j} \left(\frac{p_\eta^2}{2m_\eta} \right) \frac{\partial}{\partial x_i} = \sum_i \mathcal{B}_{i4} \frac{\partial}{\partial x_4} \left(\frac{p_\eta^2}{2m_\eta} \right) \frac{\partial}{\partial x_i}, \\
&= \mathcal{B}_{24} \frac{\partial}{\partial x_4} \left(\frac{p_\eta^2}{2m_\eta} \right) \frac{\partial}{\partial x_2} + \mathcal{B}_{34} \frac{\partial}{\partial x_4} \left(\frac{p_\eta^2}{2m_\eta} \right) \frac{\partial}{\partial x_3}, \\
&= \mathcal{B}_{24} \frac{\partial}{\partial p_\eta} \left(\frac{p_\eta^2}{2m_\eta} \right) \frac{\partial}{\partial p} + \mathcal{B}_{34} \frac{\partial}{\partial p_\eta} \left(\frac{p_\eta^2}{2m_\eta} \right) \frac{\partial}{\partial \eta}, \\
&= -p \frac{p_\eta}{m_\eta} \frac{\partial}{\partial p} + \frac{p_\eta}{m_\eta} \frac{\partial}{\partial \eta}, \qquad \text{(C.1.5)}
\end{aligned}
$$

where the splitting of the Liouville operator is

$$\mathcal{L}_1 = -\frac{\partial V(q)}{\partial q}\frac{\partial}{\partial p}, \tag{C.1.6}$$

$$\mathcal{L}_2 = \frac{p}{m}\frac{\partial}{\partial q} + \frac{p^2}{m}\frac{\partial}{\partial p_\eta}, \tag{C.1.7}$$

$$\mathcal{L}_3 = -k_B T\frac{\partial}{\partial p_\eta}, \tag{C.1.8}$$

$$\mathcal{L}_4 = -p\frac{p_\eta}{m_\eta}\frac{\partial}{\partial p} + \frac{p_\eta}{m_\eta}\frac{\partial}{\partial \eta}. \tag{C.1.9}$$

C.2 Deriving the Liouville operator for the Nosé-Hoover chain dynamics

We can find the consequent splitting of the Liouville operator from

$$\mathcal{L}_\alpha = \sum_{i,j}\mathcal{B}_{ij}\frac{\partial H_\alpha}{\partial x_j}\frac{\partial}{\partial x_i}, \tag{C.2.1}$$

Thus

$$\begin{aligned}\mathcal{L}_1 &= \sum_{i,j}\mathcal{B}_{ij}\frac{\partial H_1}{\partial x_j}\frac{\partial}{\partial x_i} = \sum_{i,j}\mathcal{B}_{ij}\frac{\partial V(q)}{\partial x_j}\frac{\partial}{\partial x_i} = \sum_i \mathcal{B}_{i1}\frac{\partial V(q)}{\partial x_1}\frac{\partial}{\partial x_i},\\ &= \mathcal{B}_{21}\frac{\partial V(q)}{\partial x_1}\frac{\partial}{\partial x_2},\\ &= -\frac{\partial V(q)}{\partial q}\frac{\partial}{\partial p},\end{aligned} \tag{C.2.2}$$

$$
\begin{aligned}
\mathcal{L}_2 &= \sum_{i,j} \mathcal{B}_{ij} \frac{\partial H_2}{\partial x_j} \frac{\partial}{\partial x_i} = \sum_{i,j} \mathcal{B}_{ij} \frac{\partial}{\partial x_j} \left(\frac{p^2}{2m} \right) \frac{\partial}{\partial x_i} = \sum_i \mathcal{B}_{i2} \frac{\partial}{\partial x_2} \left(\frac{p^2}{2m} \right) \frac{\partial}{\partial x_i}, \\
&= \mathcal{B}_{12} \frac{\partial}{\partial x_2} \left(\frac{p^2}{2m} \right) \frac{\partial}{\partial x_1} + \mathcal{B}_{42} \frac{\partial}{\partial x_2} \left(\frac{p^2}{2m} \right) \frac{\partial}{\partial x_4}, \\
&= \mathcal{B}_{12} \frac{\partial}{\partial p} \left(\frac{p^2}{2m} \right) \frac{\partial}{\partial q} + \mathcal{B}_{42} \frac{\partial}{\partial p} \left(\frac{p^2}{2m} \right) \frac{\partial}{\partial p_{\eta_1}}, \\
&= \frac{p}{m} \frac{\partial}{\partial q} + \frac{p^2}{m} \frac{\partial}{\partial p_{\eta_1}}, \qquad \text{(C.2.3)}
\end{aligned}
$$

$$
\begin{aligned}
\mathcal{L}_3 &= \sum_{i,j} \mathcal{B}_{ij} \frac{\partial H_3}{\partial x_j} \frac{\partial}{\partial x_i} = \sum_{i,j} \mathcal{B}_{ij} \frac{\partial \left(k_B T \eta_1 \right)}{\partial x_j} \frac{\partial}{\partial x_i} = \sum_i \mathcal{B}_{i3} \frac{\partial \left(k_B T \eta_1 \right)}{\partial x_3} \frac{\partial}{\partial x_i}, \\
&= \mathcal{B}_{43} \frac{\partial \left(k_B T \eta_1 \right)}{\partial x_3} \frac{\partial}{\partial x_4} = \mathcal{B}_{43} \frac{\partial \left(k_B T \eta_1 \right)}{\partial \eta_1} \frac{\partial}{\partial p_{\eta_1}}, \\
&= -k_B T \frac{\partial}{\partial p_{\eta_1}}, \qquad \text{(C.2.4)}
\end{aligned}
$$

$$
\begin{aligned}
\mathcal{L}_4 &= \sum_{i,j} \mathcal{B}_{ij} \frac{\partial H_4}{\partial x_j} \frac{\partial}{\partial x_i} = \sum_{i,j} \mathcal{B}_{ij} \frac{\partial}{\partial x_j} \left(\frac{p_{\eta_1}^2}{2m_{\eta_1}} \right) \frac{\partial}{\partial x_i} = \sum_i \mathcal{B}_{i4} \frac{\partial}{\partial x_4} \left(\frac{p_{\eta_1}^2}{2m_{\eta_1}} \right) \frac{\partial}{\partial x_i}, \\
&= \mathcal{B}_{24} \frac{\partial}{\partial x_4} \left(\frac{p_{\eta_1}^2}{2m_{\eta_1}} \right) \frac{\partial}{\partial x_2} + \mathcal{B}_{34} \frac{\partial}{\partial x_4} \left(\frac{p_{\eta_1}^2}{2m_{\eta_1}} \right) \frac{\partial}{\partial x_3} + \mathcal{B}_{64} \frac{\partial}{\partial x_4} \left(\frac{p_{\eta_1}^2}{2m_{\eta_1}} \right) \frac{\partial}{\partial x_6}, \\
&= \mathcal{B}_{24} \frac{\partial}{\partial p_{\eta_1}} \left(\frac{p_{\eta_1}^2}{2m_{\eta_1}} \right) \frac{\partial}{\partial p} + \mathcal{B}_{34} \frac{\partial}{\partial p_{\eta_1}} \left(\frac{p_{\eta_1}^2}{2m_{\eta_1}} \right) \frac{\partial}{\partial \eta_1} + \mathcal{B}_{64} \frac{\partial}{\partial p_{\eta_1}} \left(\frac{p_{\eta_1}^2}{2m_{\eta_1}} \right) \frac{\partial}{\partial p_{\eta_2}}, \\
&= -p \frac{p_{\eta_1}}{m_{\eta_1}} \frac{\partial}{\partial p} + \frac{p_{\eta_1}}{m_{\eta_1}} \frac{\partial}{\partial \eta_1} + \frac{p_{\eta_1}^2}{m_{\eta_1}} \frac{\partial}{\partial p_{\eta_2}}, \qquad \text{(C.2.5)}
\end{aligned}
$$

$$\begin{aligned}
\mathcal{L}_5 &= \sum_{i,j} \mathcal{B}_{ij} \frac{\partial H_5}{\partial x_j} \frac{\partial}{\partial x_i} = \sum_{i,j} \mathcal{B}_{ij} \frac{\partial \left(k_B T \eta_2\right)}{\partial x_j} \frac{\partial}{\partial x_i} = \sum_{i} \mathcal{B}_{i5} \frac{\partial \left(k_B T \eta_2\right)}{\partial x_5} \frac{\partial}{\partial x_i}, \\
&= \mathcal{B}_{65} \frac{\partial \left(k_B T \eta_2\right)}{\partial x_5} \frac{\partial}{\partial x_6} = \mathcal{B}_{65} \frac{\partial \left(k_B T \eta_2\right)}{\partial \eta_2} \frac{\partial}{\partial p_{\eta_2}}, \\
&= -k_B T \frac{\partial}{\partial p_{\eta_2}}, \qquad \text{(C.2.6)}
\end{aligned}$$

$$\begin{aligned}
\mathcal{L}_6 &= \sum_{i,j} \mathcal{B}_{ij} \frac{\partial H_6}{\partial x_j} \frac{\partial}{\partial x_i} = \sum_{i,j} \mathcal{B}_{ij} \frac{\partial}{\partial x_j} \left(\frac{p_{\eta_2}^2}{2m_{\eta_2}} \right) \frac{\partial}{\partial x_i} = \sum_{i} \mathcal{B}_{i6} \frac{\partial}{\partial x_6} \left(\frac{p_{\eta_2}^2}{2m_{\eta_2}} \right) \frac{\partial}{\partial x_i}, \\
&= \mathcal{B}_{46} \frac{\partial}{\partial p_{\eta_2}} \left(\frac{p_{\eta_2}^2}{2m_{\eta_2}} \right) \frac{\partial}{\partial x_4} + \mathcal{B}_{56} \frac{\partial}{\partial p_{\eta_2}} \left(\frac{p_{\eta_2}^2}{2m_{\eta_2}} \right) \frac{\partial}{\partial x_5}, \\
&= -p_{\eta_1} \frac{p_{\eta_2}}{m_{\eta_2}} \frac{\partial}{\partial p_{\eta_1}} + \frac{p_{\eta_2}}{m_{\eta_2}} \frac{\partial}{\partial \eta_2}. \qquad \text{(C.2.7)}
\end{aligned}$$

As a consequence of the splitting of the Hamiltonian, the corresponding Liouville pieces are

$$\begin{aligned}
\mathcal{L}_1 &= -\frac{\partial V\left(q\right)}{\partial q} \frac{\partial}{\partial p}, \qquad \text{(C.2.8)} \\
\mathcal{L}_2 &= \frac{p}{m} \frac{\partial}{\partial q} + \frac{p^2}{m} \frac{\partial}{\partial p_{\eta_1}}, \qquad \text{(C.2.9)} \\
\mathcal{L}_3 &= -k_B T \frac{\partial}{\partial p_{\eta_1}}, \qquad \text{(C.2.10)} \\
\mathcal{L}_4 &= -p \frac{p_{\eta_1}}{m_{\eta_1}} \frac{\partial}{\partial p} + \frac{p_{\eta_1}}{m_{\eta_1}} \frac{\partial}{\partial \eta_1} + \frac{p_{\eta_1}^2}{m_{\eta_1}} \frac{\partial}{\partial p_{\eta_2}}, \qquad \text{(C.2.11)} \\
\mathcal{L}_5 &= -k_B T \frac{\partial}{\partial p_{\eta_2}}, \qquad \text{(C.2.12)} \\
\mathcal{L}_6 &= -p_{\eta_1} \frac{p_{\eta_2}}{m_{\eta_2}} \frac{\partial}{\partial p_{\eta_1}} + \frac{p_{\eta_2}}{m_{\eta_2}} \frac{\partial}{\partial \eta_2}. \qquad \text{(C.2.13)}
\end{aligned}$$

C.3 Deriving the Liouville operator for the Bulgac-Kusnezov dynamics

We can find the consequent splitting of the Liouville operator from

$$\mathcal{L}_\alpha = \sum_{i,j} \mathcal{B}_{ij} \frac{\partial H_\alpha}{\partial x_j} \frac{\partial}{\partial x_i}, \tag{C.3.1}$$

Thus, for a system with one degree of freedom, coordinate q, momentum p and mass m,

$$\begin{aligned} L_1 &= \sum_{i,j} \mathcal{B}_{ij} \frac{\partial H_1}{\partial x_j} \frac{\partial}{\partial x_i} = \sum_{i,j} \mathcal{B}_{ij} \frac{\partial V(q)}{\partial x_j} \frac{\partial}{\partial x_i} = \sum_i \mathcal{B}_{i1} \frac{\partial V(q)}{\partial x_1} \frac{\partial}{\partial x_i}, \\ &= \mathcal{B}_{41} \frac{\partial V(q)}{\partial x_1} \frac{\partial}{\partial x_4} + \mathcal{B}_{61} \frac{\partial V(q)}{\partial x_1} \frac{\partial}{\partial x_6}, \\ &= F \frac{\partial}{\partial p} - qF \frac{\partial}{\partial p_\xi}, \end{aligned} \tag{C.3.2}$$

$$\begin{aligned} L_2 &= \sum_{i,j} \mathcal{B}_{ij} \frac{\partial H_2}{\partial x_j} \frac{\partial}{\partial x_i} = \sum_{i,j} \mathcal{B}_{ij} \frac{\partial}{\partial x_j} \left(\frac{p_i^2}{2m_i} \right) \frac{\partial}{\partial x_i} = \sum_i \mathcal{B}_{i2} \frac{\partial}{\partial x_2} \left(\frac{p_i^2}{2m_i} \right) \frac{\partial}{\partial x_i}, \\ &= \mathcal{B}_{52} \frac{\partial}{\partial x_2} (k_B T \eta) \frac{\partial}{\partial x_5}, \\ &= \frac{p}{m} \frac{\partial}{\partial q} + \frac{p^2}{m} \frac{\partial}{\partial p_\zeta}, \end{aligned} \tag{C.3.3}$$

$$
\begin{aligned}
L_3 &= \sum_{i,j} \mathcal{B}_{ij} \frac{\partial H_3}{\partial x_j} \frac{\partial}{\partial x_i} = \sum_{i,j} \mathcal{B}_{ij} \frac{\partial}{\partial x_j} \left(k_B T \chi\right) \frac{\partial}{\partial x_i} = \sum_{i} \mathcal{B}_{i3} \frac{\partial}{\partial x_3} \left(k_B T \chi\right) \frac{\partial}{\partial x_i}, \\
&= \mathcal{B}_{63} \frac{\partial}{\partial x_3} \left(k_B T \chi\right) \frac{\partial}{\partial x_6}, \\
&= -k_B T \frac{\partial}{\partial p_\zeta}, \qquad \text{(C.3.4)}
\end{aligned}
$$

$$
\begin{aligned}
L_4 &= \sum_{i,j} \mathcal{B}_{ij} \frac{\partial H_4}{\partial x_j} \frac{\partial}{\partial x_i} = \sum_{i,j} \mathcal{B}_{ij} \frac{\partial}{\partial x_j} \left(\frac{p^2}{2m}\right) \frac{\partial}{\partial x_i} = \sum_{i} \mathcal{B}_{i4} \frac{\partial}{\partial x_4} \left(\frac{p^2}{2m}\right) \frac{\partial}{\partial x_i}, \\
&= \mathcal{B}_{14} \frac{\partial}{\partial x_4} \left(\frac{p^2}{2m}\right) \frac{\partial}{\partial x_1} + \mathcal{B}_{54} \frac{\partial}{\partial x_4} \left(\frac{p^2}{2m}\right) \frac{\partial}{\partial x_5}, \\
&= -k_B T \frac{\partial}{\partial p_\xi}, \qquad \text{(C.3.5)}
\end{aligned}
$$

$$
\begin{aligned}
L_5 &= \sum_{i,j} \mathcal{B}_{ij} \frac{\partial H_5}{\partial x_j} \frac{\partial}{\partial x_i} = \sum_{i,j} \mathcal{B}_{ij} \frac{\partial}{\partial x_j} \left(\frac{p_\eta^2}{2M_\eta}\right) \frac{\partial}{\partial x_i} = \sum_{i} \mathcal{B}_{i5} \frac{\partial}{\partial x_5} \left(\frac{p_\eta^2}{2M_\eta}\right) \frac{\partial}{\partial x_i}, \\
&= \mathcal{B}_{25} \frac{\partial}{\partial x_5} \left(\frac{p_\eta^2}{2M_\eta}\right) \frac{\partial}{\partial x_2} + \mathcal{B}_{45} \frac{\partial}{\partial x_5} \left(\frac{p_\eta^2}{2M_\eta}\right) \frac{\partial}{\partial x_4} + \mathcal{B}_{65} \frac{\partial}{\partial x_5} \left(\frac{p_\eta^2}{2M_\eta}\right) \frac{\partial}{\partial x_6}, \\
&= \frac{p_\zeta}{m_\zeta} \frac{\partial}{\partial \zeta} - \frac{p_\zeta}{m_\zeta} p \frac{\partial}{\partial p}, \qquad \text{(C.3.6)}
\end{aligned}
$$

$$
\begin{aligned}
L_6 &= \sum_{i,j} \mathcal{B}_{ij} \frac{\partial H_6}{\partial x_j} \frac{\partial}{\partial x_i} = \sum_{i,j} \mathcal{B}_{ij} \frac{\partial}{\partial x_j} \left(\frac{p_\chi^2}{2M_\chi}\right) \frac{\partial}{\partial x_i} = \sum_{i} \mathcal{B}_{i6} \frac{\partial}{\partial x_6} \left(\frac{p_\chi^2}{2M_\chi}\right) \frac{\partial}{\partial x_i}, \\
&= \mathcal{B}_{36} \frac{\partial}{\partial x_6} \left(\frac{p_\chi^2}{2M_\chi}\right) \frac{\partial}{\partial x_3} + \mathcal{B}_{56} \frac{\partial}{\partial x_6} \left(\frac{p_\chi^2}{2M_\chi}\right) \frac{\partial}{\partial x_5}, \\
&= \frac{p_\xi}{m_\xi} \frac{\partial}{\partial \xi} - \frac{p_\xi}{m_\xi} q \frac{\partial}{\partial q}. \qquad \text{(C.3.7)}
\end{aligned}
$$

Consequently we have the Liouville operator as

$$\mathcal{L}_1 = -\frac{\partial V(q)}{\partial q}\frac{\partial}{\partial p} + q\frac{\partial V(q)}{\partial q}\frac{\partial}{\partial p_\xi}, \tag{C.3.8}$$

$$\mathcal{L}_2 = \frac{p}{m}\frac{\partial}{\partial q} + \frac{p^2}{m}\frac{\partial}{\partial p_\zeta}, \tag{C.3.9}$$

$$\mathcal{L}_3 = -k_B T\frac{\partial}{\partial p_\zeta}, \tag{C.3.10}$$

$$\mathcal{L}_4 = -k_B T\frac{\partial}{\partial p_\xi}, \tag{C.3.11}$$

$$\mathcal{L}_5 = \frac{p_\zeta}{m_\zeta}\frac{\partial}{\partial \zeta} - \frac{p_\zeta}{m_\zeta}p\frac{\partial}{\partial p}, \tag{C.3.12}$$

$$\mathcal{L}_6 = \frac{p_\xi}{m_\xi}\frac{\partial}{\partial \xi} - \frac{p_\xi}{m_\xi}q\frac{\partial}{\partial q}. \tag{C.3.13}$$

Bibliography

[1] D. Frenkel and B. Smit, *Understanding Molecular simulation: From Algorithms to Applications* (Academic, New York, 2001).

[2] H. Fehske, R. Schneider and A. Weibe, *Computational Many-Particle Physics* (Springer, Berlin Heidelberg, 2008).

[3] D. C. Rapaport, *The art of molecular dynamics simulation* (Cambridge University press, Cambridge, 1995).

[4] A. Sergi and P. V. Giaquinta, J. Stat. Mech. **2007**, P02013 (2007).

[5] A. Sergi and M. Ferrario, Phys. Rev. E **64**, 056125 (2001).

[6] S. Nosé, Mol. Phys. **52**, 255 (1984).

[7] S. Nosé, Prog. Theor. Phys. **103**, 1 (1991).

[8] S. Nosé, J. Chem. Phys. **81**, 511 (1984).

[9] S. Nosé, Mol. Phys. **57**, 187 (1986).

[10] H. C. Andersen, J. Chem. Phys. **72**, 2384 (1980).

[11] P. Klein, Modell. Simul. Mater. Sci. Eng. **6**, 405 (1998).

[12] W. G. Hoover, Phys. Rev. A **34**, 2499 (1986).

[13] J. Jellinek, J. Chem. Phys. **92**, 3163 (1988).

[14] A. Bulgac and D. Kusnezov, Phys. Rev. A **42**, 5045 (1990).

[15] A. Sergi, Phys. Rev. E **67**, 021101 (2003).

[16] M. Tuckerman, G. J. Martyna and B. J. Berne, J. Chem. Phys. **97**, 1990 (1992).

[17] M. Suzuki, J. Math. Phys. **26**, 601 (1985).

[18] E. Forest and R. D. Ruth, Physica D **43**, 105 (1990).

[19] A. Sergi and G. Ezra, AAPP **88**, 2 (2010).

[20] G. S. Ezra, J. Chem. Phys. **125**, 034104 (2006).

[21] M. P. Allen and D. J. Tildesley, *Computer simulation of liquids* (Oxford University press, Oxford, 1988).

[22] D. J. Evans and G. P. Morriss, *Statistical mechanics of Non-equilibrium liquids* (Academic, New York, 1990).

[23] B. Leimkuler and S. Reich, *Simulating Hamiltonian Dynamics* (Cambridge University Press, Cambridge, 2004).

[24] M. E. Tuckerman, *Statistical Mechanics : Theory and Molecular simulation* (Oxford University Press, Oxford, 2002).

[25] H. Goldstein, *Classical Mechanics* (Addison-Wesley, London, 1980).

[26] R. Balescu, *Equilibrium and Nonequilibrium statistical mechanics* (Wiley, New York, 1975).

[27] J. E. Marsden and T. S. Ratiu, *Introduction to Mechanics and Symmetry* (Springer-Verlag, New York, 1999).

[28] D. Beeman, J. Comp. Phys. **20**, 130 (1976).

[29] D. Levesque and L. Verlet, J. Stat. Phys. **72**, 519 (1993).

[30] G. Ciccotti and W. G. Hoover, *Molecular Dynamics Simulation of Statistical Mechanical Systems* (North-Holland, Amsterdam, 1986).

[31] L. Verlet, Phys. Rev. **159**, 98 (1967).

[32] W. C. Swope, H. C. Andersen, P. H. Berens, and K. R. Wilson, J. Chem. Phys **76**, 637 (1982).

[33] W. G. Hoover, Phys. Rev. A **31**, 1695 (1985).

[34] G. J. Martyna, M. L. Klein and M. Tuckerman, J. Chem. Phys. **92**, 2635 (1992).

[35] M. Tuckerman, C. J. Mundy and G. J. Martyna, Europhys. Lett. **45**, 149 (1999).

[36] P. J. Morrison, Rev. Mod. Phys. **70**, 467 (1998).

[37] J. L. McCauley, *Classical Mechanics* (Cambridge University Press, Cambridge, 1997).

[38] A. Bulgac and D. Kusnezov, Ann. Phys. **199**, 187 (1990).

[39] D. Kusnezov and A. Bulgac, Ann. Phys. **214**, 180 (1992).

[40] D. Kusnezov, A. Bulgac and W. Bauer, Ann. Phys. **204**, 155 (1990).

[41] A. Sergi, M. Ferrario and D. Costa, Mol. Phys. **97**, 825 (1999).

[42] G. J. Martyna, M. Tuckerman, D. J. Tobias and M. L. Klein, Mol. Phys. **87**, 1117 (1996).

[43] A. Sergi and G. Ezra, Phys. Rev. E **81**, 036705 (2010).